Res.

FC

Technical Report

to the

Office of Naval Research

On

ADSORPTION FROM SOLUTION OF STEARIC ACID ON IRON; EFFECT ON ELECTRODE POTENTIAL

by

Norman Hackerman and John J. Bordeaux

November 23, 1956

Contract Nonr - 375(02)

Department of Chemistry
The University of Texas

Austin, Texas

Introduction

Sorption from solution onto metal surfaces is of interest from the standpoint of fundamental surface chemistry and also from the more practical viewpoint of lubrication, corrosion inhibition, and catalysis. The effect of electrochemically inactive solutes on irreversible, steady state potentials is of interest from the standpoint of the fundamental characteristics of electrode processes as well as from the more practical viewpoint of corrosion reactions. There are numerous accounts of researches in which the adsorption and the electrochemical effects have been measured on the same material but in general has been in different physical form for the two kinds of experiments, e.g., powder and sheet respectively.

A more desirable state of affairs would obtain if both kinds of measurements could be made on the bulk metal itself. The principal difficulty lies in determining the extent, and rate, of adsorption, on the inherently low surface area materials. Two possible ways of overcoming this difficulty are (i) to develop very precise and sensitive methods for analysis of the solutions, e.g., spectrophotometric; and (ii) to use compounds into which a suitable radioisotope can be incorporated. The work reported here followed the latter course.

C^{14}-tagged stearic acid was used as the adsorbate and high purity ironas the sorbent and electrode. Because the solubility of stearic acid in water is too low to provide a suitable working range of concentrations the solvent used was 80% ethanol-20% water. Solution conductivity was maintained suitably by adding sodium perchlorate as a solute also.

Experimental

The ethanol was U. S. Industrial Chemical Company absolute alcohol (b.p. 78.4°C.) and the water was double distilled. G. Frederick Smith sodium perchlorate was used without purification as the electrolyte. The non-radioactive stearic acid used was Eastman Kodak Company practical grade and was recrystallized from ethanol twice (m.p. 68.7°C.). The radioactive stearic acid, C-14 carboxyl-labeled, was obtained from Tracerlab Inc. and had a specific activity of 1 millicurie per millimole. This material was reported to have a melting point from 67.4° to 68.2°C., this was checked and found to be 68.4°C. The radioactive stearic acid was used as received. It was obtained under license of the Atomic Energy Commission.

Preparation of Solutions:

A stock solution of 1 M Na ClO_4 was prepared and from this a second stock solution of 8×10^{-3} M stearic acid in 1 M Na ClO_4 was prepared. The following solutions were prepared by dilution of the stearic acid-containing

stock by the stearic acid-free stock, thus all contained 1 M Na ClO_4; 10^{-3}, 8×10^{-4}, 6×10^{-4}, 5×10^{-4}, 4×10^{-4}, 2×10^{-4}, 8×10^{-5}, 4×10^{-5} and 10^{-5}M.

The radioactive stearic acid solutions were prepared in the same manner as were the non-radioactive solutions. The stock solution contained 7.5×10^{-3} moles per liter and the following solutions were prepared from it by dilution; 3×10^{-3}, 10^{-3}, 7×10^{-4}, 4×10^{-4}, 10^{-4}, and 5×10^{-5}M.

Other Materials:

The design of the electrodes is discussed under apparatus. The iron used was Armco Steel Corporation high purity iron, their analysis on the material being: C - 0.010%, Mn - 0.010%, P - 0.005%, S - 0.012%, Si - 0.002%, and Cu - 0.040%.

The iron specimens used as sorbents were discs of the same material as the electrodes. They had a radius of 0.96 + 0.01 cm., were approximately 1/16 inch thick, and were polished to knife-like edges.

The gas used to maintain an air-free atmosphere was grade A helium from the Amarillo Division of the Bureau of Mines. They report this gas to be 99.997 percent pure with not more than 10^{-6} percent oxygen or water vapor.

Standard commercial grade oxygen was used where required.

All other chemicals used were of reagent grade.

Apparatus and Procedure

Potential Measuring System:

The experimental cell shown in Figure 1 is approximately 2/3 actual size. The iron test electrode (A) was screwed onto a teflon plug (B). For the detail of the electrode assembly see Figure 2a. In the latter figure note the small diameter tip (1 mm dia.) with a 0.35 mm. diameter capillary (D). This is similar to the "backside capillary" described by Barnartt (1) and in detail by Eisenberg, Tobias, and Wilke (2). A tapped hole (C), Figure 2a, was used to connect a brass rod (C), Figure 1, to the iron test electrode. The teflon plug was pressure fitted into a glass tube to form a solution bridge (D). A coating of Myvawax was then applied to the sides of the electrode, the exposed teflon collar, the end of the glass tube and the brass lead. Only the face of the electrode was left exposed. The auxiliary polarizing electrode was a platinized platinum wire spiral sealed in glass and was placed in a sidearm well (E). The stopcock (ungreased) between the well and the main part of the cell was maintained in a partially opened position. A gas inlet tube (F) admitted the helium into the cell through a porous disc (H). The gas then passed out of the cell through the outlet tube (G) and thence through a bubble trap to prevent the back flow of oxygen into the system.

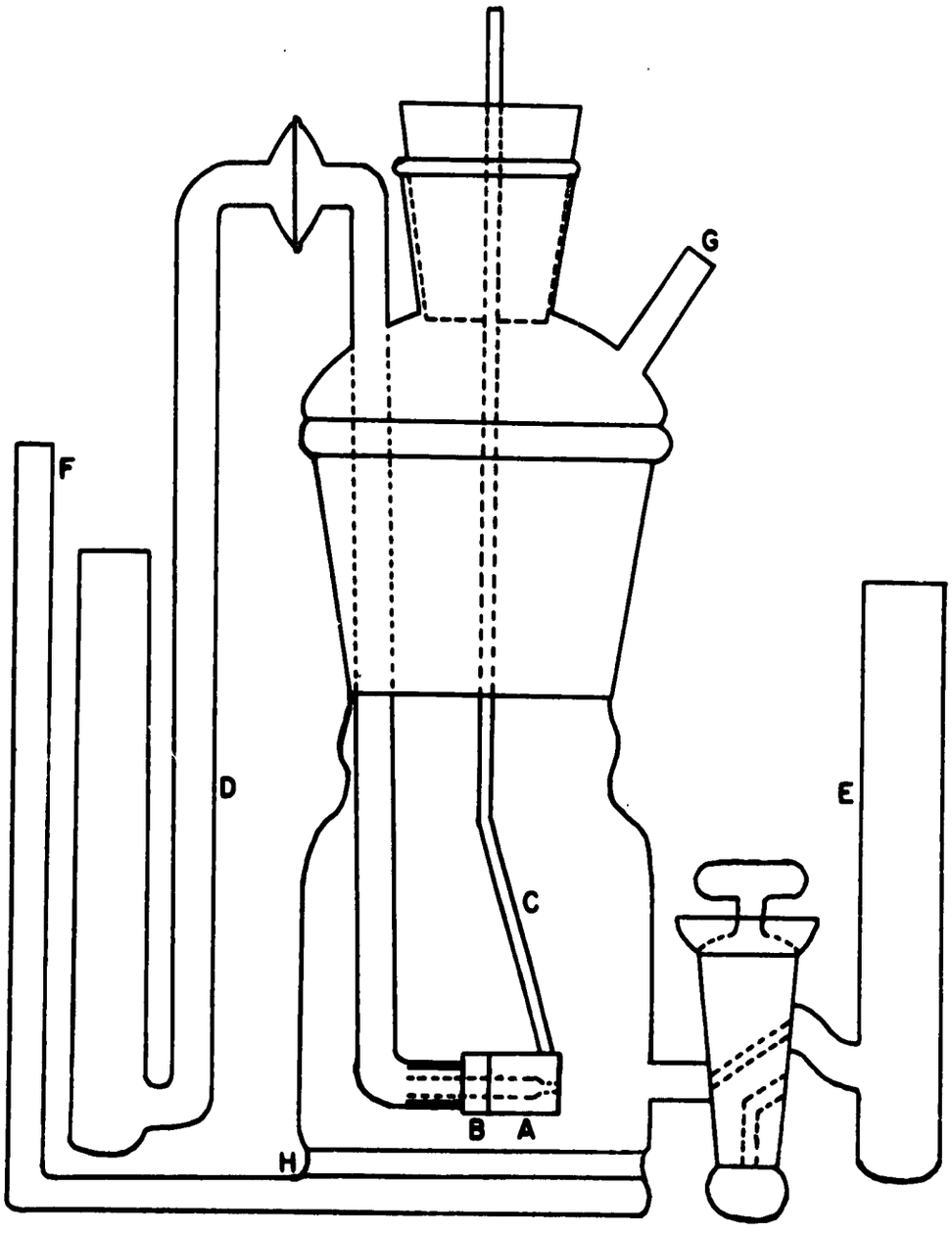

Figure 1

x ell

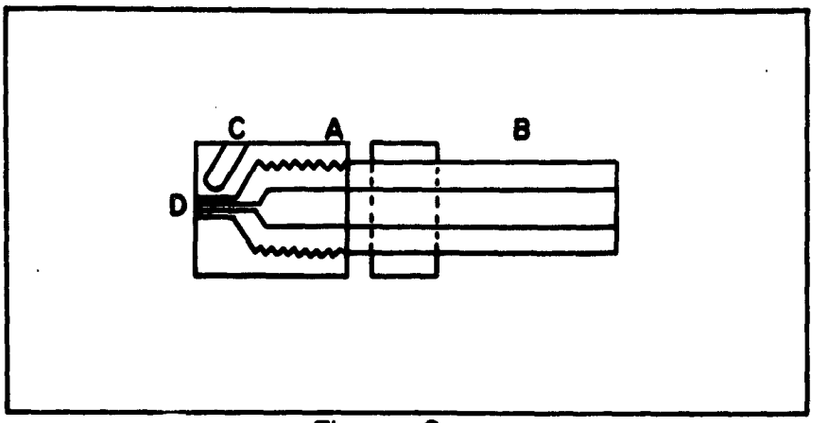

Figure 2a

Backside capillary and electrode detail.

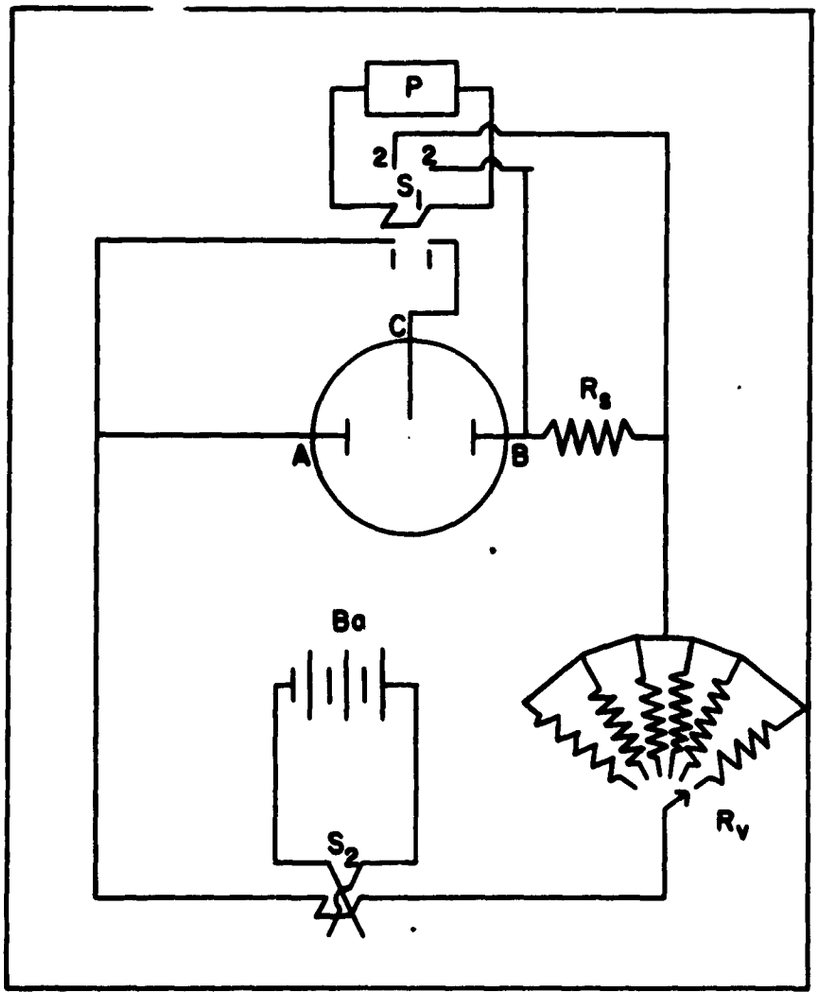

Figure 2b

Schematic diagram of the electrical circuit.

Preliminary experiments were performed using a different electrode arrangement. The tip of the capillary (dia. 0.5 mm.) was placed even with the front edge and at a distance of about four times the capillary radius from the test electrode surface. It is difficult to measure accurately the error introduced by an ohmic drop in the solution with this type of arrangement. However, the potentials measured in this way and with the backside capillary did not differ by more than 5 mv. for the current densities employed. Barnartt's work indicates that with solutions of conductivity similar to those used here, the correctionfor ohmic resistance of the solution should be only a few millivolts. The backside capillary system was used because it introduced a smaller correction factor and yielded more reproducible results.

A schematic diagram of the circuit is shown in Figure 2b. It consisted of a simple potentiometric circuit (P) for measuring the potential drop between the test electrode (A) and a saturated calomel reference electrode (C). The potentiometer circuit was replaced by a Minneapolis Honeywell, Brown Electronik recording potentiometer model Y 153 12 V - X - (IV) for obtaining the potential-time traces on anodic polarization. For open circuit potential measurements, switch (S_1) was placed in position 1 and switch (S_2) was open. In polarization runs, the direction of the current flow could be reversed by placing switch (S_2) in either position this allowing either cathodic or anodic polarization. The polarizing circuit consisted of the iron test electrode (A) in series with a platinized platinum non-polarizable electrode (B), a precision resistance (R_s) calibrated to one percent, a variable resistance (R_v), and a 45 volt battery in the circuit through the reversing switch (S_2). By varying the resistance in (R_v) the current passing through the cell could be controlled at several values and could be determined by measuring the potential drop across the precision resistance (R_s) with the potentiometer.

The procedure for the open circuit potential determination was to fill the cell with the solution in question; bubble solvent saturated helium through the system; insert the electrode and periodically measure the potential until a steady state was obtained, 24 hours usually being sufficient.

In the polarization experiments, the above procedure was followed until steady state was attained and then the current was applied. Time was allowed for the electrode to reach a steady state potential at each current density. The time necessary on anodic polarization was from 8 to 15 minutes, but for cathodic polarization, the time was from 30 to 60 minutes in neutral unbuffered solutions or 5 minutes in buffered or acid solutions. All polarization experiments were carried out at 25 $\pm$ 1°C.

Adsorption System and Counting Procedure and Instruments:

The adsorption system was similar to that described by Stephens (3). The adsorption tube was a 25 x 100 mm. test tube with a gas inlet tube in the bottom. A short section of 22 mm. O. D. glass tubing was cut so as to have one end at 90° to its linear axis and the other at 30°. The 30° end had several small glass ears, each pointing toward the center, and another

on the short linear edge. This was inserted in the adsorption tube to serve as a support for the specimen. A cork stopper was fitted with a gas outlet tube and inserted in the test tube. These tubes could be mounted in a series with helium flowing from the more dilute to the more concentrated. The helium was presaturated with solvent to prevent loss by evaporation.

The adsorption operation was carried out inside a dry box under a helium atmosphere. The procedure was to evacuate the dry box using a water aspirator, cut off the suction with a pinch clamp and fill the dry box with helium to a slight positive pressure. This procedure was repeated twice and then the solvent saturated helium was bubbled through the adsorption tubes for an hour. The iron discs were placed in the tubes and the bubbling of helium continued. The total time allowed for adsorption was 24 hours. This length of time was used so that the time allowed for the electrodes to reach a steady state open circuit potential and the time allowed for adsorption was the same. The adsorption was carried out at temperatures of 25 $\pm$ 1 and 30 $\pm$ 1°C.

The coupons were removed from solution with a pair of long pointed nickel tweezers. The coupon was taken out of the tube quickly and the edge touched against a piece of facial tissue.

The desorption or removal of the stearic acid not irreversibly absorbed was accomplished by repeated washings with nearly boiling absolute alcohol, then with nearly boiling benzene, and finally by refluxing with benzene in a soxhlet extractor for several hours. This process was repeated until counting data showed no decrease in the quantity remaining on the coupon.

The counting of the active stearic acid adsorbed on the specimens was carried out using a Tracerlab Model S C 16 Windowless Geiger Flow Counter except for those few cases of very high activity. These were counted in a standard, thin mica window counter; a factor was predetermined to allow conversion of these results onto the same basis as those obtained with the flow counter. Background counts were taken periodically during the counting operation and were never found to be more than 25 counts per minute. A count of at least 10,000 was always taken; this gives a standard deviation of one percent. Each specimen was counted at least six times and the reproducibility of each series was better than 5 percent.

Preparation of the Electrode and Sorbent Surfaces:

The electrode and sorbent surfaces were annealed at 1000°C in a vacuum of 10^{-5} mm. of Hg for 1 hour. They were then polished before each experiment with number 2 emery paper and cleaned by degreasing with benzene. All specimens were stored in a vacuum desiccator under a helium atmosphere until used. The diameter from which the apparent area was calculated was determined after each experiment using a traveling microscope.

Measurements of pH:

The pH of the solutions used in polarization experiments was measured before and after each run with a Beckman model G pH meter.

Results

Open Circuit Potentials:

The open circuit potential of iron, whether in a solution containing stearic acid or in 1 M $NaClO_4$, changed with time. The change as shown in Figure 3 was in the increasingly active direction first, passing through a maximum and then a minimum, finally leveling off after about 16 hours. Appendix I gives typical data taken over about a 24 hour period. All potentials are given relative to the saturated calomel electrode.

The change in potential with concentration in an air-free system at 25°C. is shown in Figure 4, curve A, and the data are given in Appendix II. Curve B of Figure 4 is the same as curve A except that oxygen was being bubbled through the system instead of helium. The ΔE scale (farthest right) represents the difference between the open circuit potential of a stearic acid-free system and the open circuit potential of one containing a given amount of stearic acid. These potentials versus concentration experiments were carried out at three temperatures, 30°C., 25°C., and 15°C. Figure 5 shows the effect of temperature, also Appendix II.

Adsorption Measurements:

The adsorption of stearic acid onto iron is partially reversible and partially irreversible. The total amount of stearic acid adsorbed as a function of solution concentration at 25°C. and 30°C. is given in Figure 6 and the data are in Appendix III. Figure 7 shows the amount irreversibly held (left) and the surface coverage in monolayers (right) at 25°C. and 30°C. See also Appendix III.

It may be seen from Figure 8 that the point at which leveling off begins is approximately the same for both ΔE and q, i.e., at between 0.8 and 1 mM.

Polarization Measurements:

The anodic and cathodic polarization curves for various systems are shown in Figures 9 and 14, and the data are given in Appendix IV. In these plots, ΔE_c and ΔE_a represent the measured potential change from open circuit due to the passing of current, either cathodic or anodic. The curves in Figure 9 represent measurements made in neutral solution of varying stearic acid concentrations from 0 to 8×10^{-3} M and with no buffer present. Those in Figure 14 are for measurements of systems in 0.1N $HClO_4$ (pH 1), and of systems containing buffer (pH 6.5).

Figure 3

Potential-Time Traces for Open Circuit

From Time of Immersion to Steady State

Solutions:

1. 1 M $NaClO_4$
2. .04 mM Stearic Acid + 1 M $NaClO_4$
3. .08 mM Stearic Acid + 1 M $NaClO_4$
4. .20 mM Stearic Acid + 1 M $NaClO_4$
5. .40 mM Stearic Acid + 1 M $NaClO_4$
6. .80 mM Stearic Acid + 1 M $NaClO_4$
7. 8.0 mM Stearic Acid + 1 M $NaClO_4$

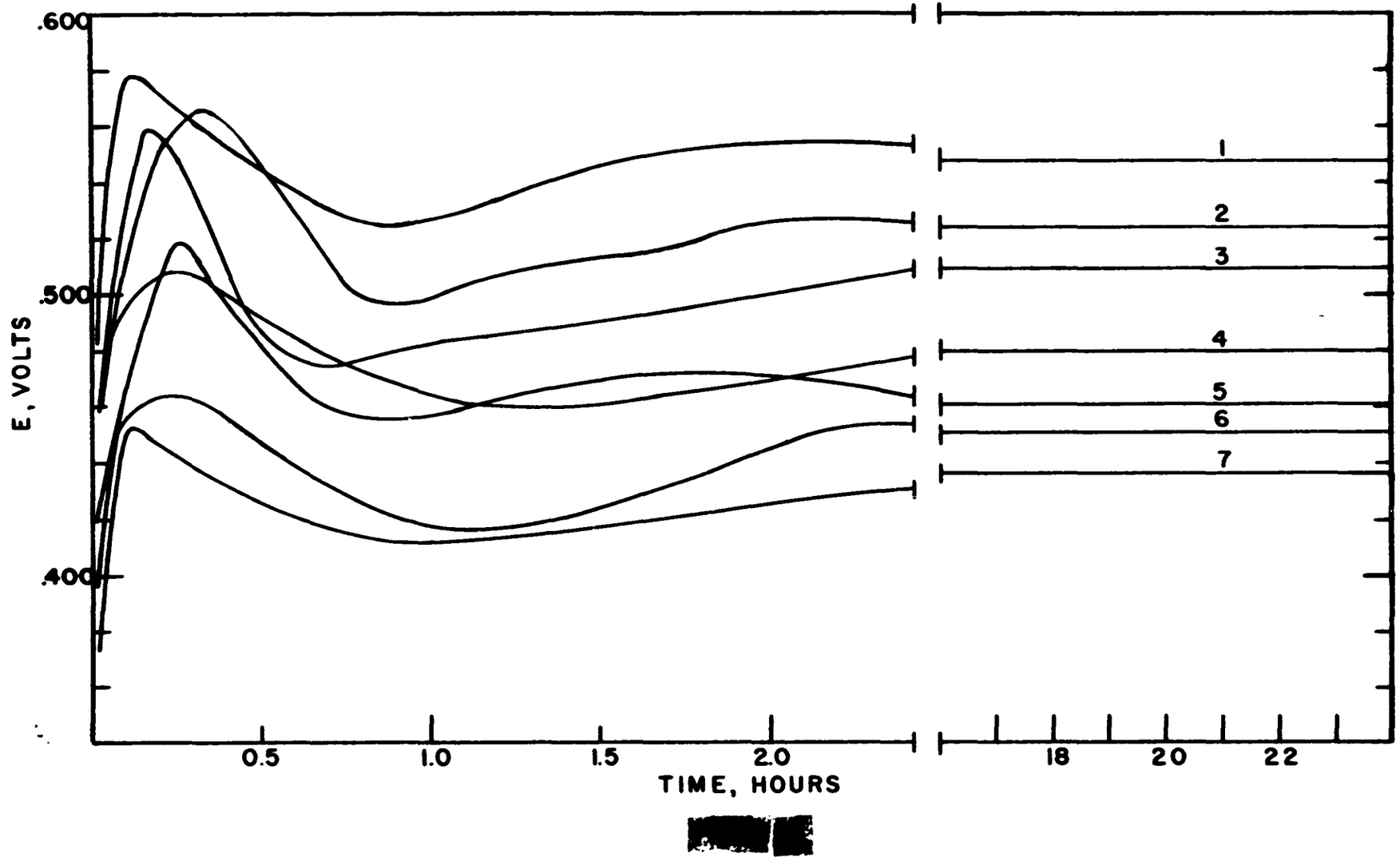
.600
.500
.400
E, VOLTS
1
2
3
4
5
6
7
0.5
1.0
1.5
2.0
18
20
22
TIME, HOURS

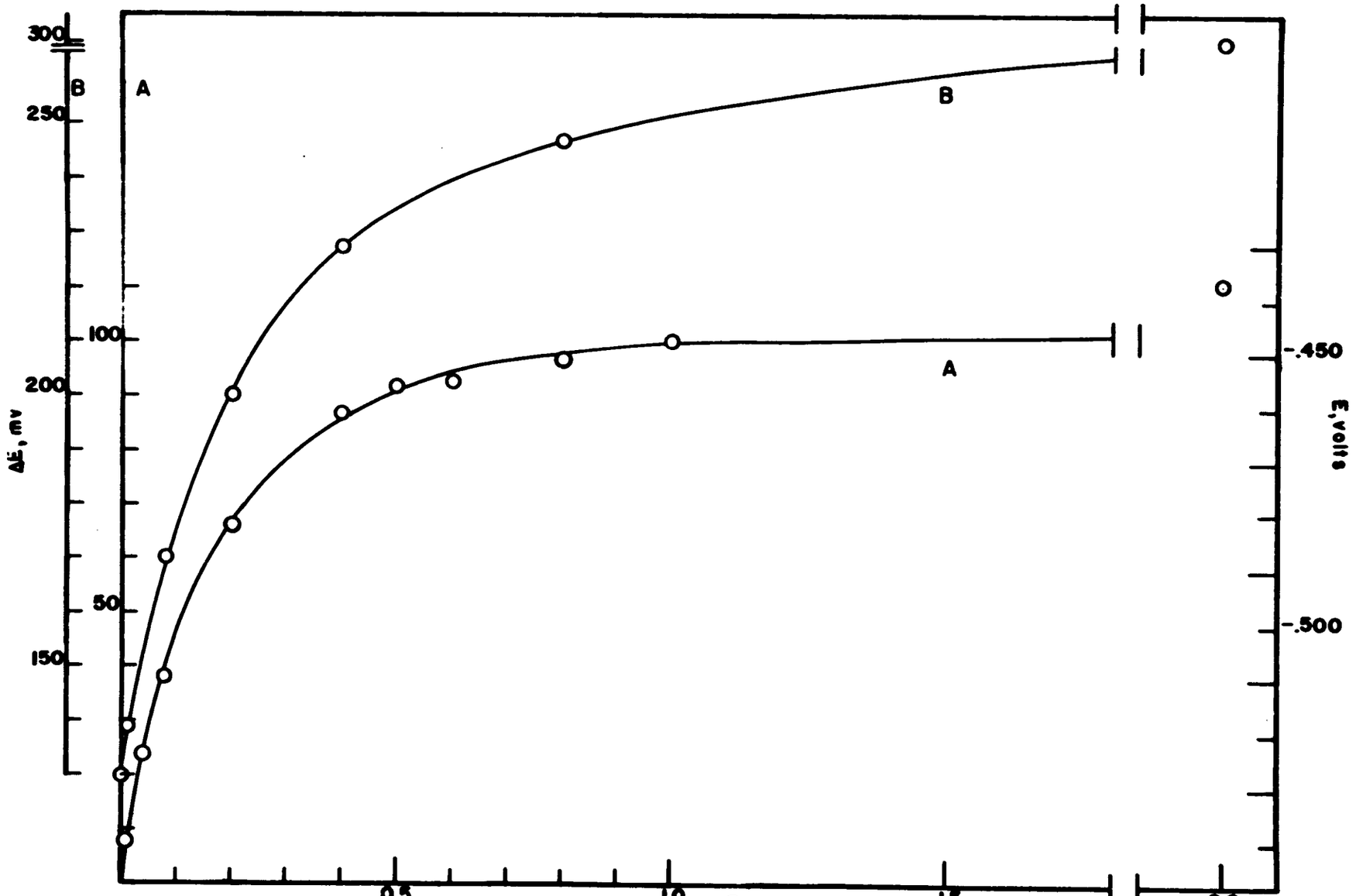

Curve A Potential vs concentration of stearic acid in air-free solutions.

[illegible] 4

Curve B Potential vs concentration of stearic acid in oxygen saturated solutions.

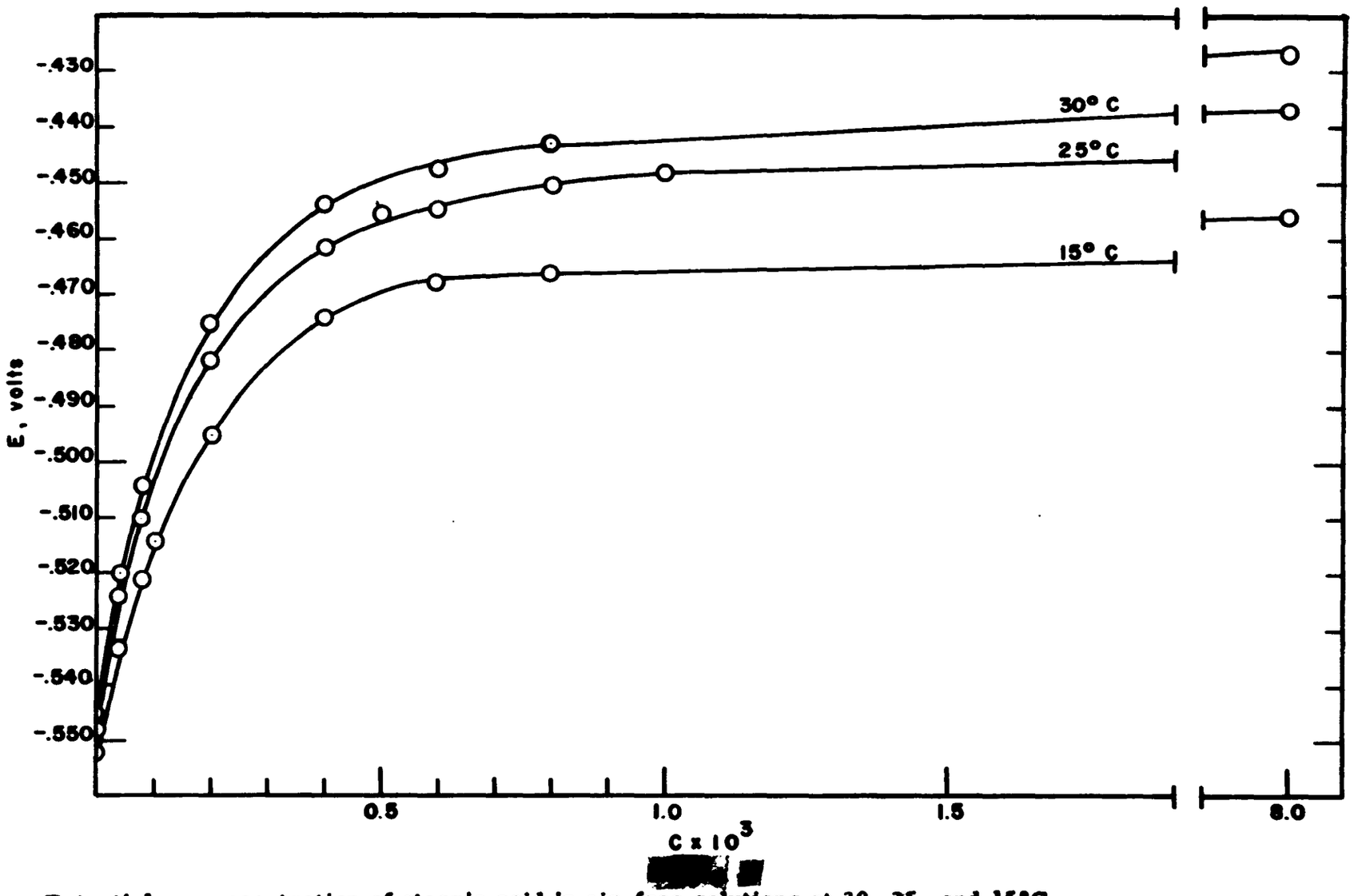

Potential vs concentration of stearic acid in air-free solutions at 30, 25, and 15°C.

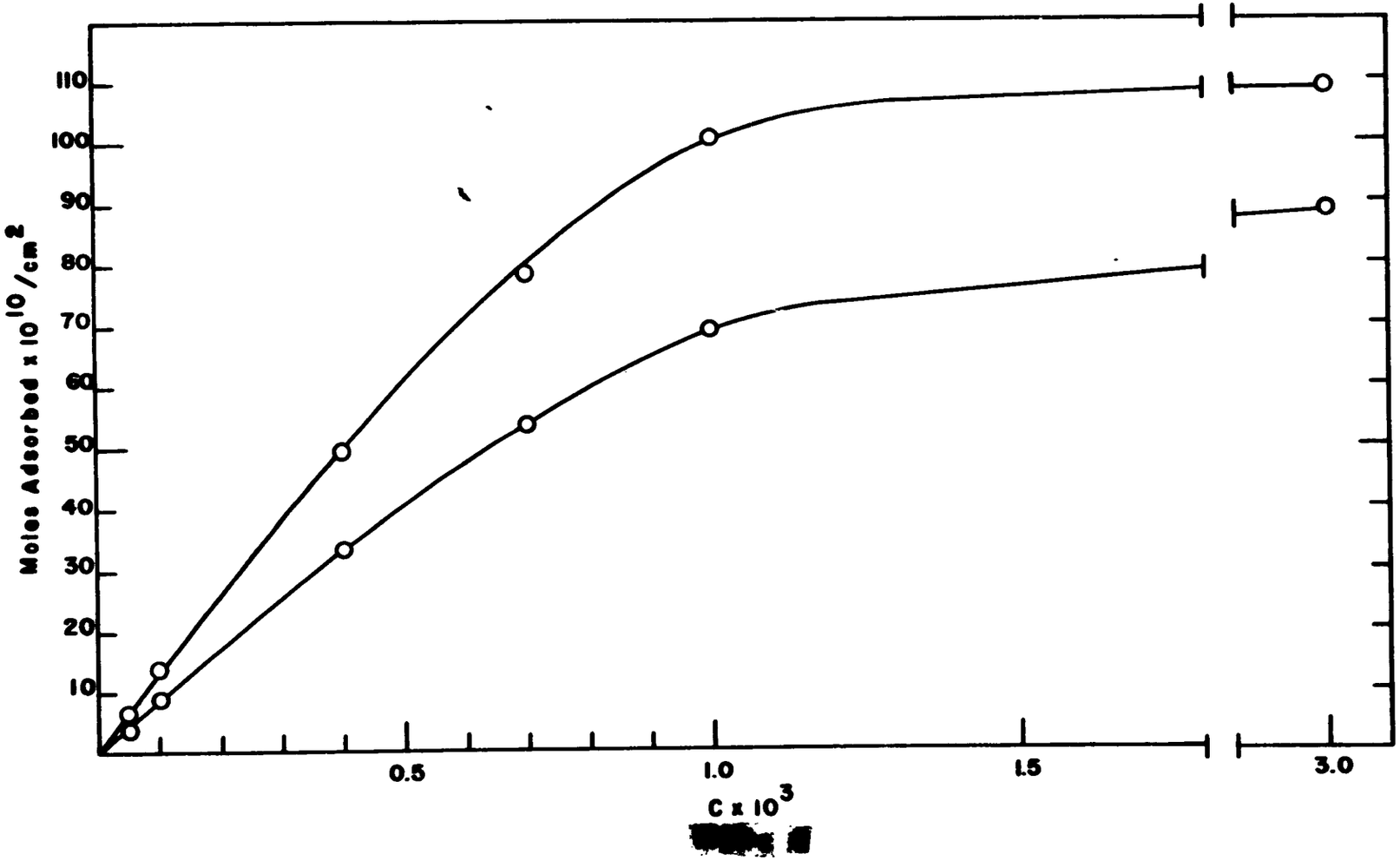

Total adsorption of stearic acid on iron.

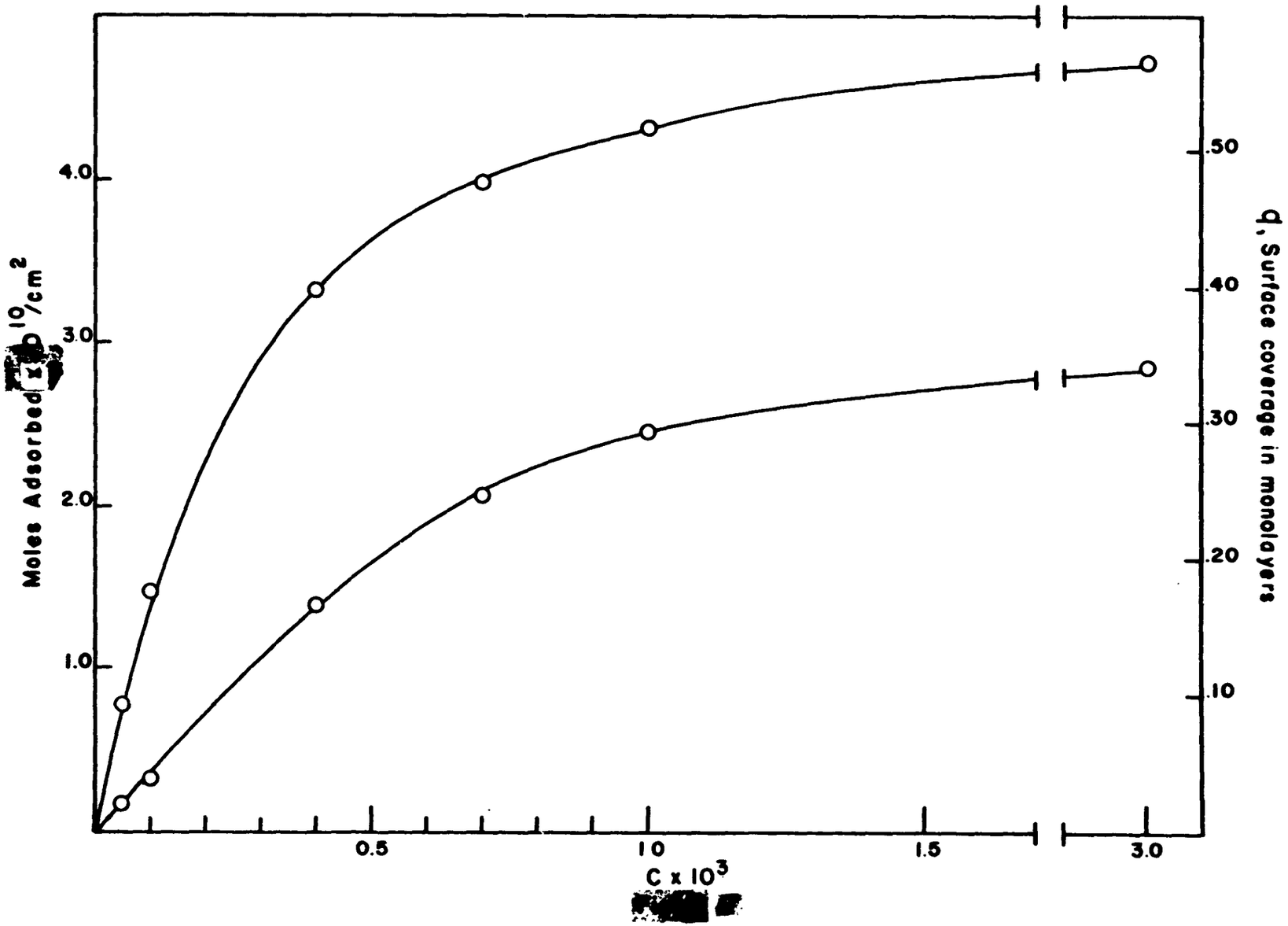

Chemisorption of stearic acid on iron.

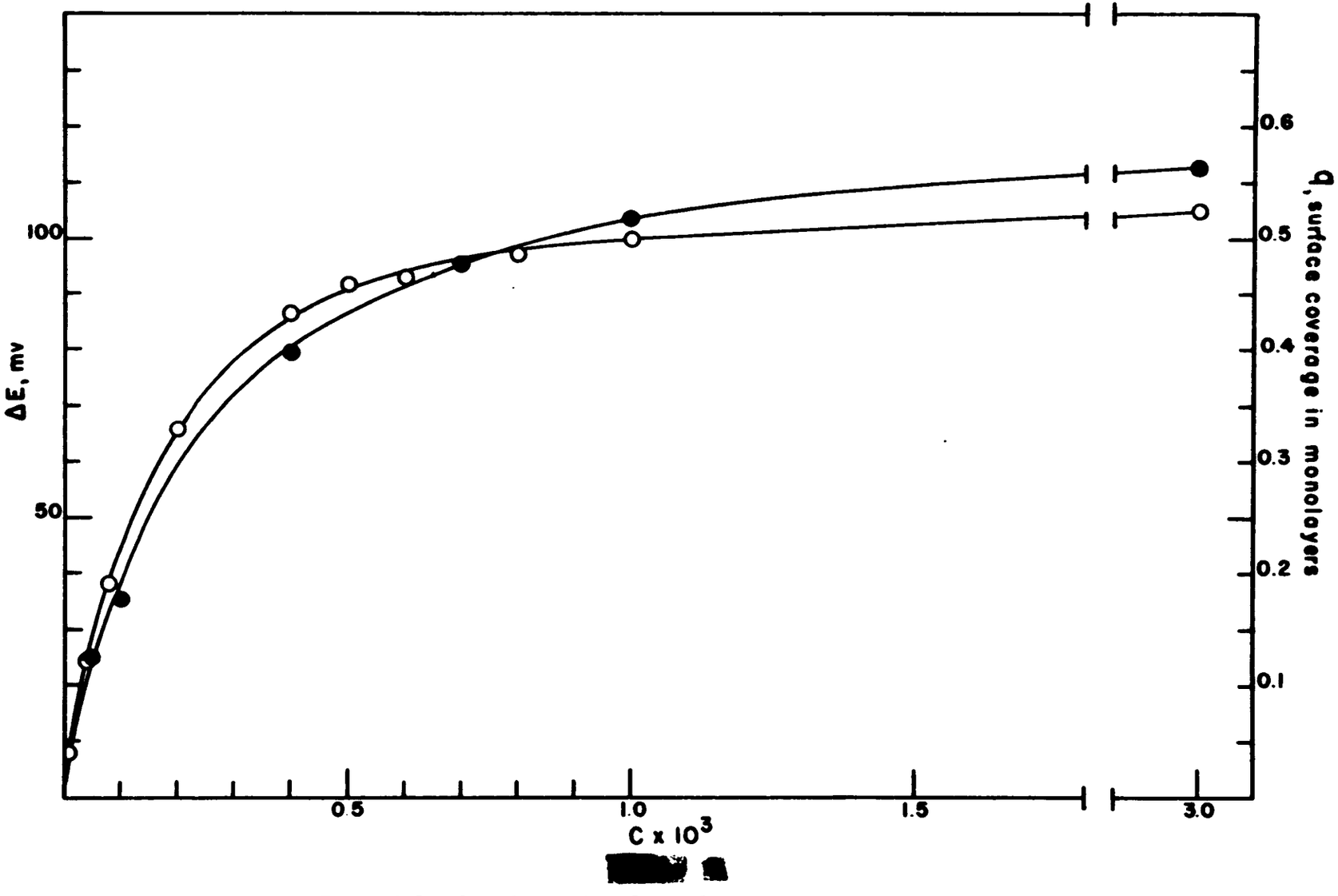

Potential, chemisorption dependency on concentration.

Figure 9

Potential vs Current Density

ΔE_c, change in cathodic potential
i_c, cathodic current density
ΔE_c, change in anodic potential
i_c, anodic current density

Solutions

1 and 1a	1 M $NaClO_4$
2 and 2a	8.0 mM Stearic Acid + 1 M $NaClO_4$
3 and 3a	0.8 mM Stearic Acid + 1 M $NaClO_4$
4 and 4a	0.5 mM Stearic Acid + 1 M $NaClO_4$

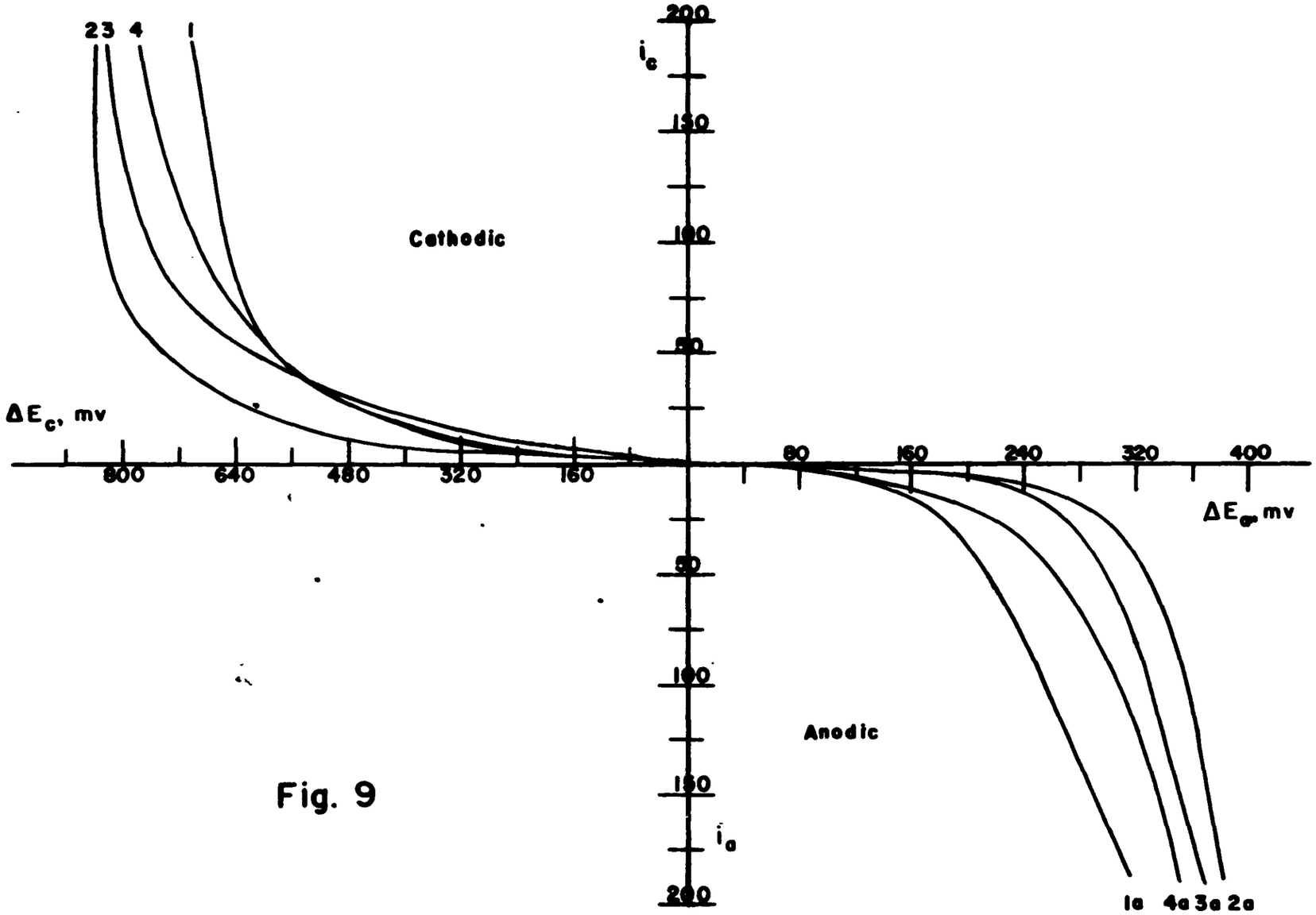
23 4 1
200
i_c
150
100
50
Cathodic
ΔE_c, mv
800
640
480
320
160
80
160
240
320
400
ΔE_a, mv
50
100
Anodic
150
i_a
200
1a 4a 3a 2a

Fig. 9

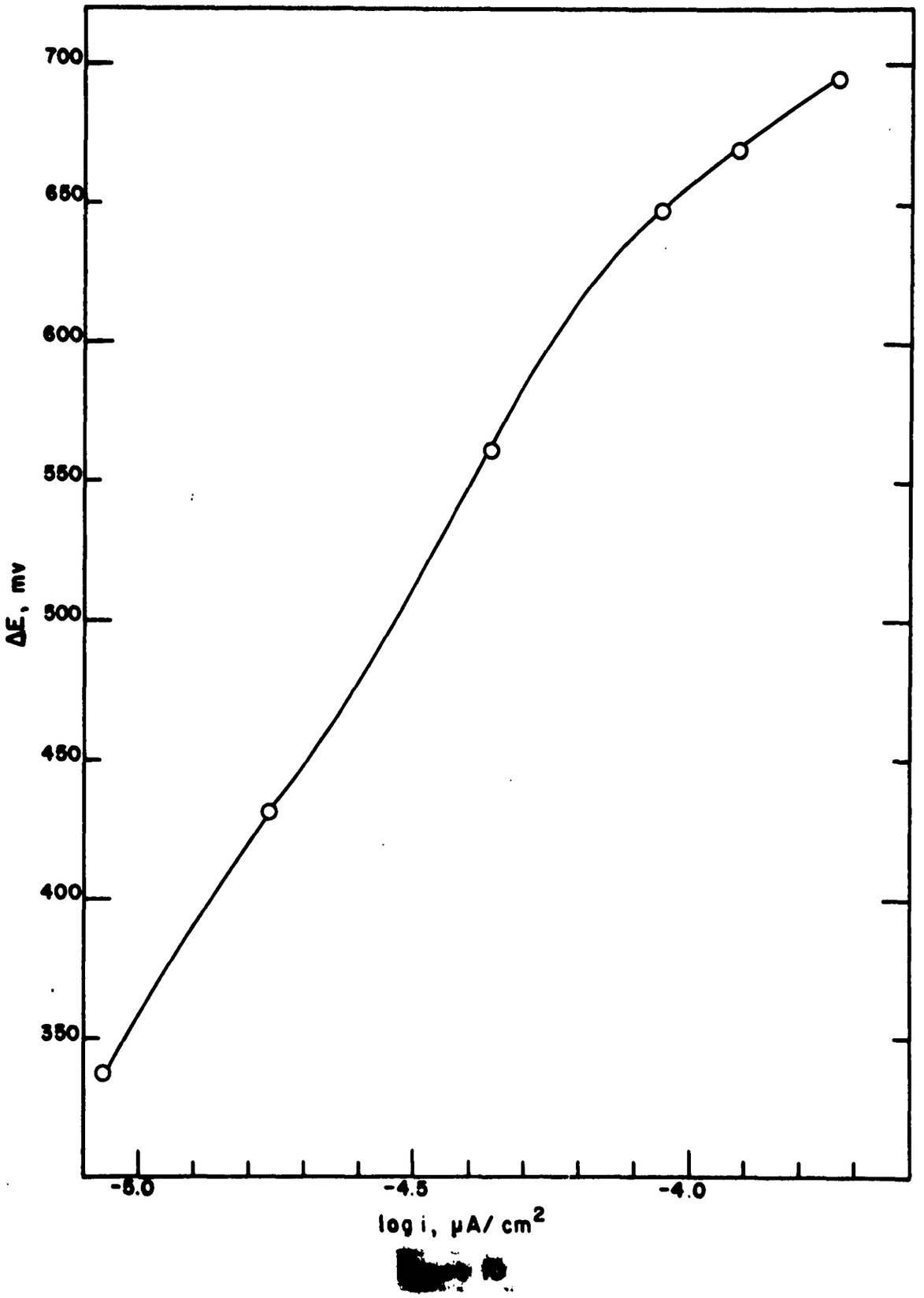

Cathodic overpotential vs log i. Solution: 1 M $NaClO_4$
(Data from curve 1, figure 9)

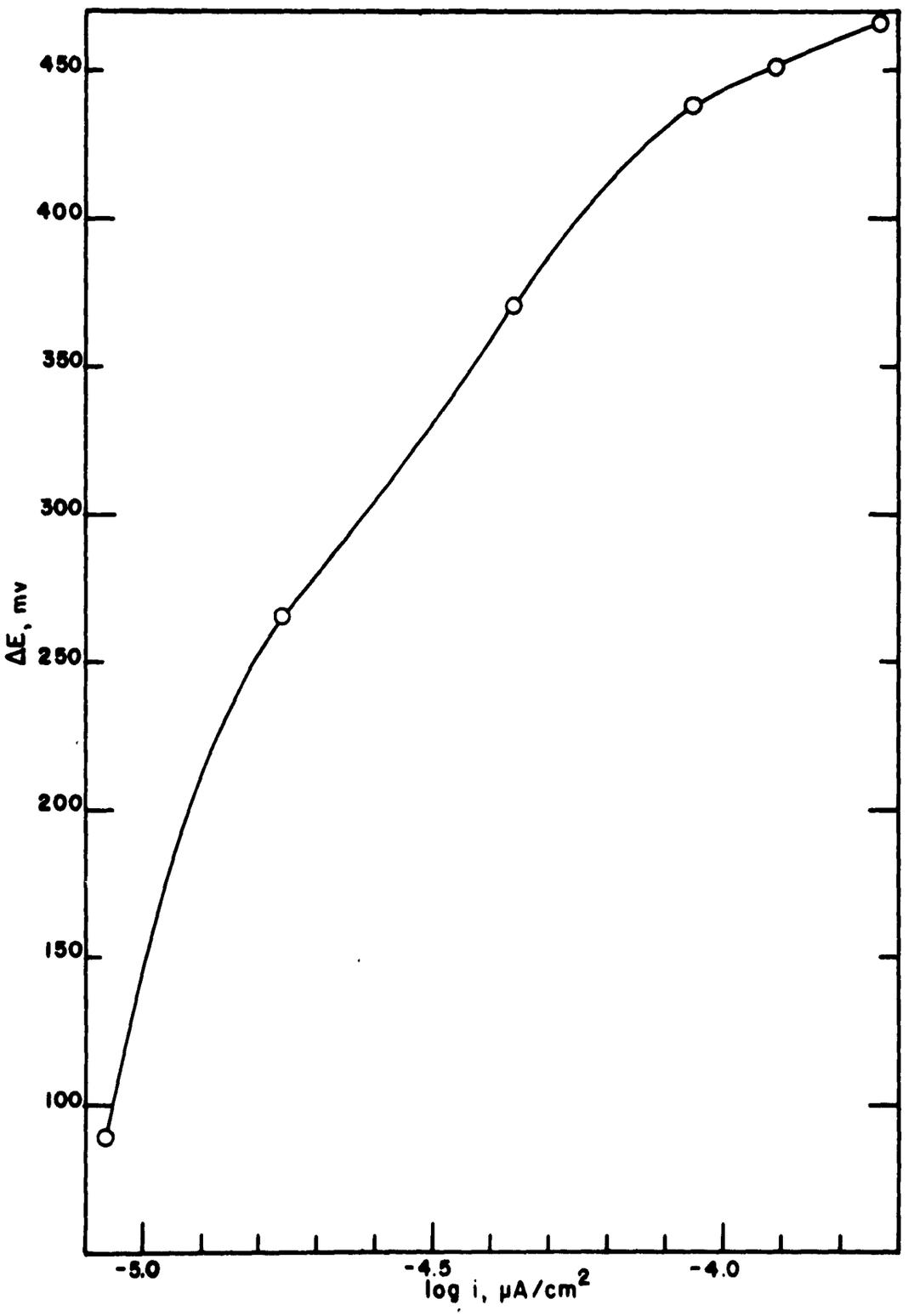

Figure

Corrected cathodic overpotential vs log i.
Solution: 1 M $NaClO_4$

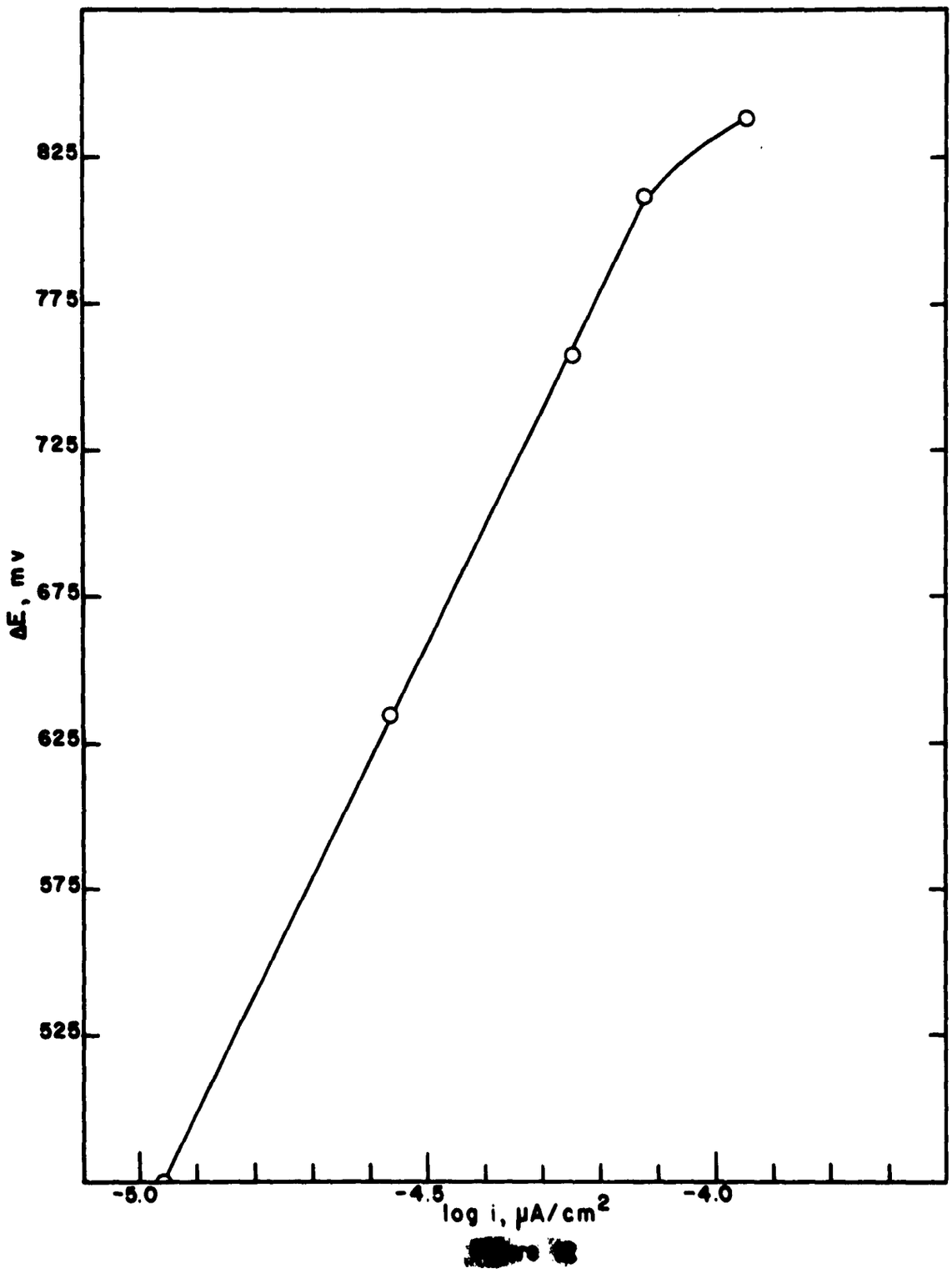

Cathodic overpotential vs log. i.
Solution: 8.0 mM stearic acid + 1 M $NaClO_4$
(Data from curve 2, figure 9)

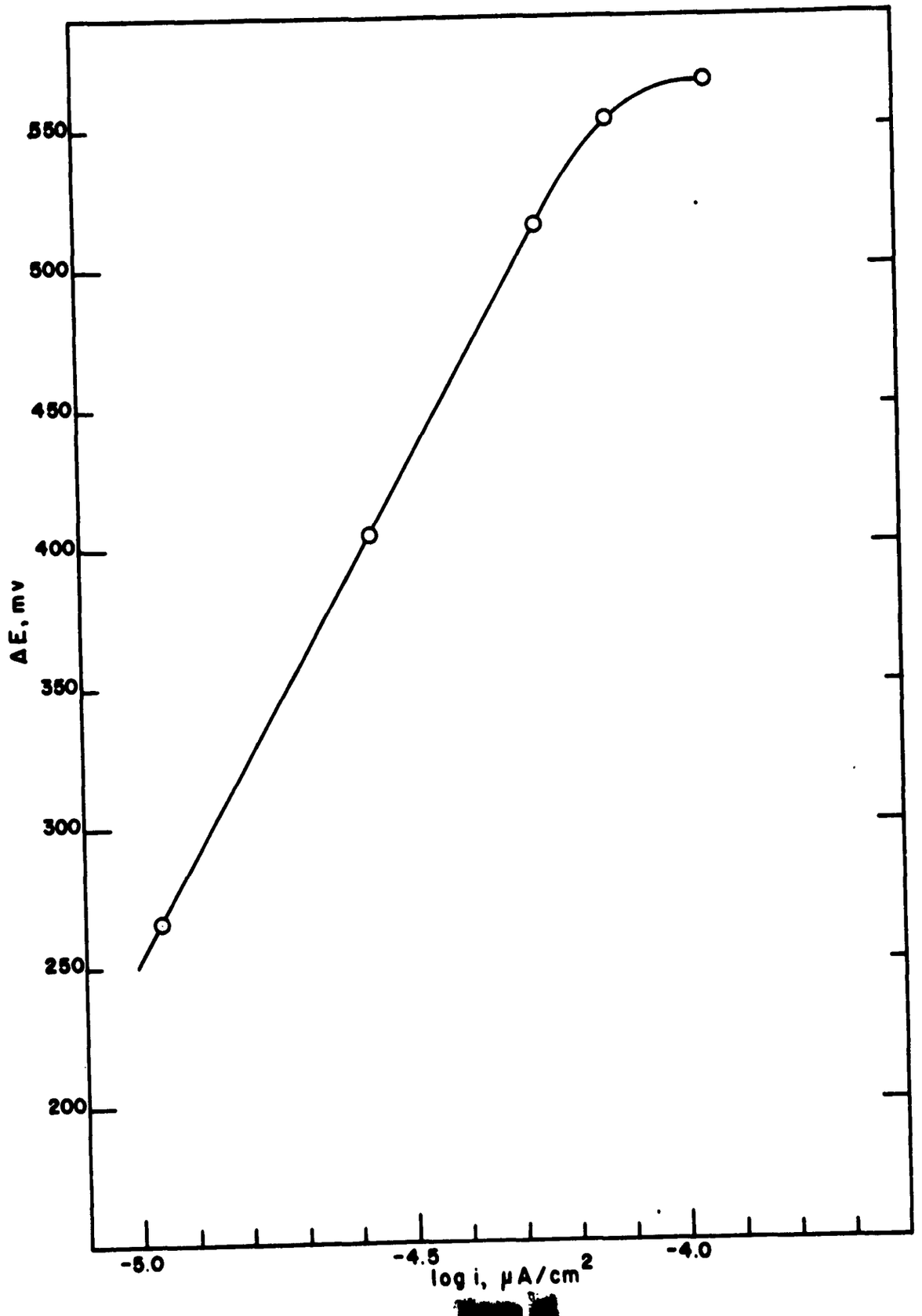

Corrected cathodic overpotential vs log i.
Solution: 8.0 mM stearic acid + 1 M $NaClO_4$

Figure 14

Potential vs Current Density

ΔE_c, change in cathodic potential

ic, cathodic current density

ΔE_a, change in anodic potential

ia, anodic current density

Solutions:

1 and 1 a	0.1 N $HClO_4$
2 and 2a	0.1 N $HClO_4$ + 1 M $NaClO_4$
3 and 3a	8.0 mM Stearic Acid + 0.1 N $HClO_4$ + 1 M $NaClO_4$
4 and 4a	1 M $NaClO_4$ + Acetic Acid-Sodium Acetate Buffer
5 and 5a	1 M $NaClO_4$ + Propionic Acid-Sodium Propionate Buffer
6 and 6a	1 M $NaClO_4$ + Butyric Acid-Sodium Butyrate Buffer

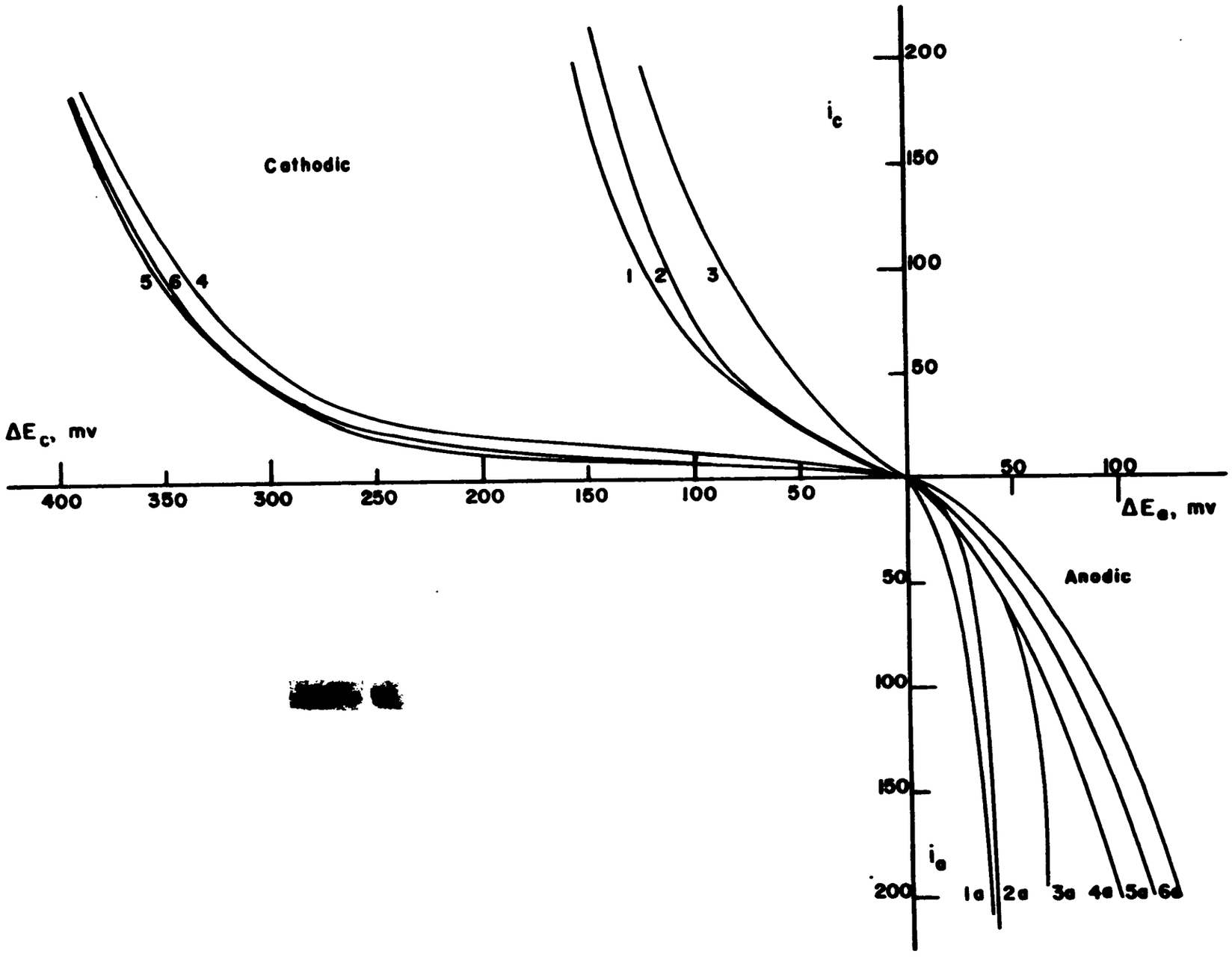
Cathodic
i_c
200
150
100
50
1 2 3
5 6 4
ΔE_c, mv
400 350 300 250 200 150 100 50
50 100
ΔE_a, mv
Anodic
50
100
150
i_a
200
1a 2a 3a 4a 5a 6a

Figures 10 and 12 are curves for ΔE_c versus log i using the experimental values for potential change as observed. Figures 11 and 13 are curves for the same data with the ΔE values corrected (see discussion). Figures 12 and 13 are typical of the data obtained in the presence of stearic acid; complete tables are given in Appendix IV.

Figure 15 is a Tafel plot of change in potential ΔE_c against log current density. In this, the current density is based on the apparent area rather than the true area. The apparent area was used because of the unknown extent of surface area change brought about by metal dissolution under an applied potential.

Figure 16 shows two typical time potential plots at particular current densities on anodic polarization.

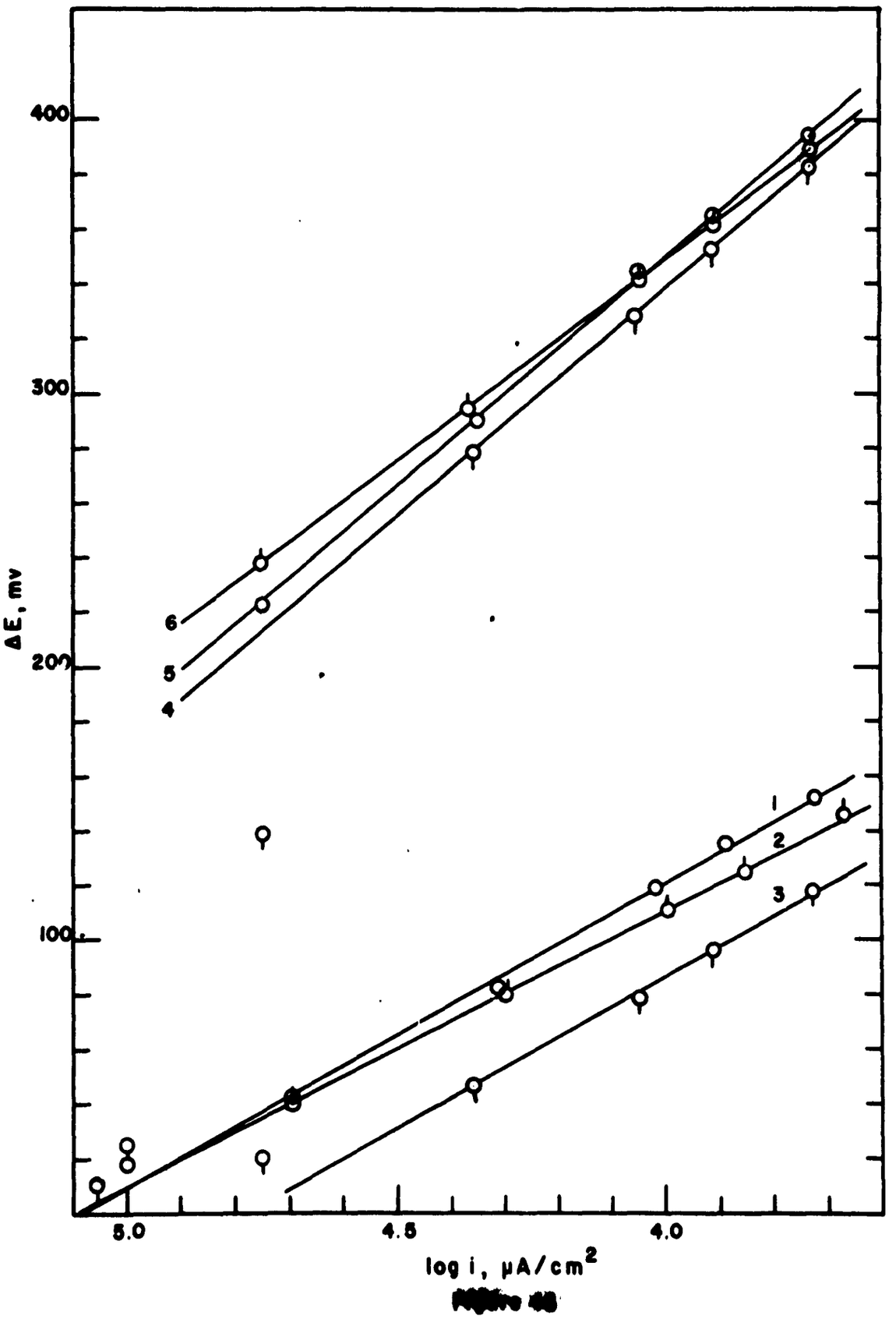
400
300
200
100
ΔE, mv
6
5
4
1
2
3
5.0
4.5
4.0
log i, μA/cm²

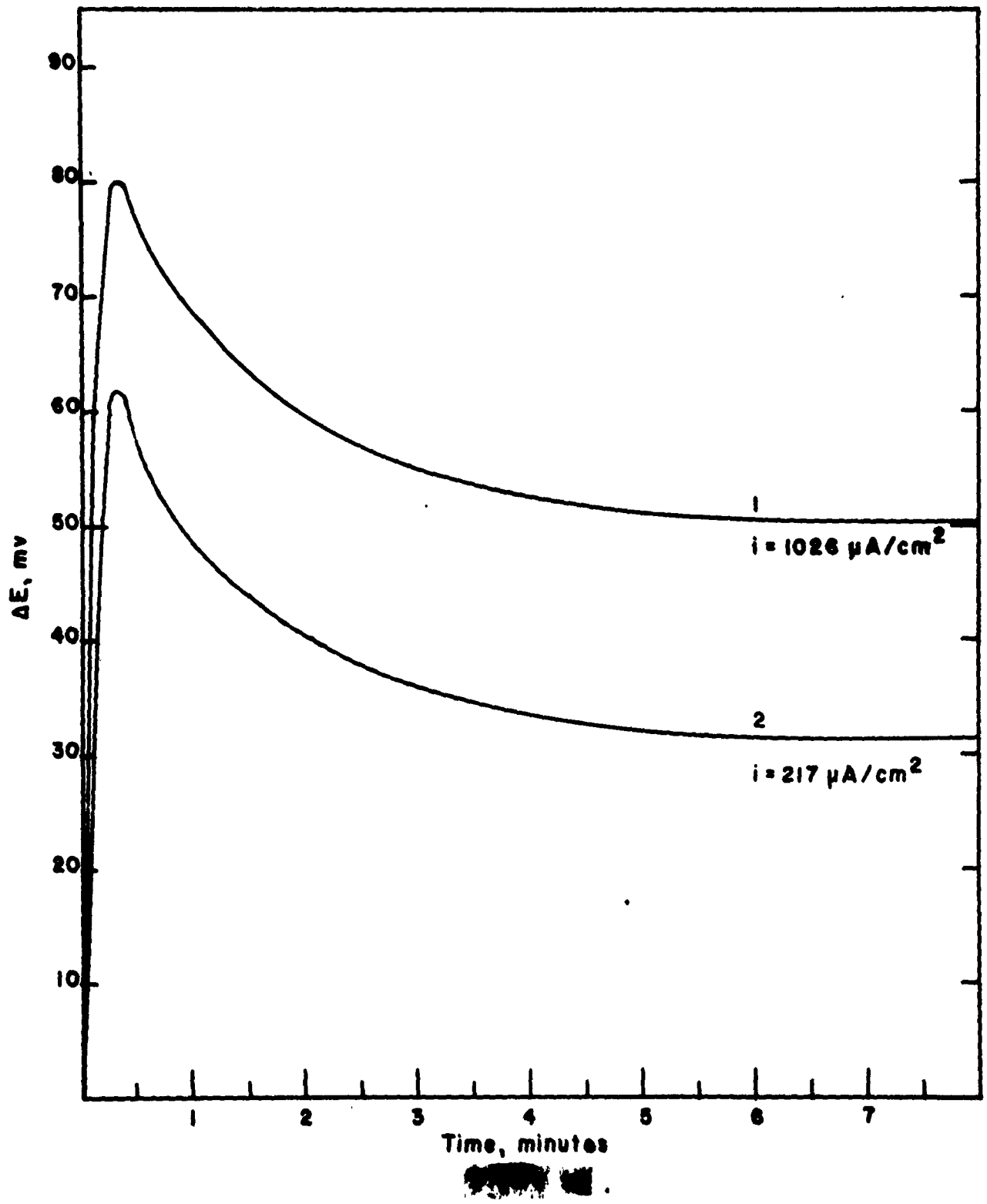

i = Applied anodic current.

Discussion

Adsorption:

Studies on the adsorption of stearic acid on powdered steel have been reported by Hackerman and Cook (4, 5) and by Roebuck (6). The latter used a tracer technique similar to the one used in this work as well as the gravimetric method used by Hackerman and Cook.

The total amount of stearic acid adsorbed on the iron surface is considerably higher than that found in the above investigations, see Table 1. However, they were carried out in pure benzene solutions while the present work is in a mixed solvent in which the solubility of stearic acid is much lower than in benzene. There is also a high concentration of sodium perchlorate present. Furthermore, there may be some differences in the amount adsorbed due to the differences between pure iron and steel. Such differences between similar systems are discussed by Morris and Holister (7) who investigated the adsorption of stearic and other acids on different types of carbon black using different solvents. They found considerable variation in the quantities of stearic acid adsorbed.

It is likely that the differences caused by the latter effect are small since the amount of chemisorbed stearic acid on iron compares favorably with that found by gravimetric methods. However, the amount found here was again higher than that reported by Roebuck (6) for irreversible adsorption using the tracer technique, Table 1.

Adsorption, both total and chemisorbed, decreases as temperature increases. This behavior is normal and negative temperature coefficients are usually observed. Isotherms at 25 and 30°C. for both total and chemisorption are shown in Figures 6 and 7 respectively.

The surface coverage in monolayers of chemisorbed stearic acid as a function of concentration is also shown in Figure 7 (ordinate on right). In calculating the surface covered, a value of 20.5 $\AA^2$ was used as the area per molecule. This is the value given by Kipling (8) and by Vold (9). Graham and Hansen (10) recently reported values for the area covered by an acid molecule as between 22 and 38 $\AA^2$. The explanation for this range is: "At a coverage below $\theta = 0.78$, the indicated molecular area was 38 $\AA^2$ or about the same as butane. This suggests that the molecules lie flat on the surface with the two oxygen atoms occupying about the same area as $-CH_2-$ groups. At higher coverages, the molecular area drops to 22 $\AA^2$ or approximately that of ethane." However, in their work, carbon was the sorbent and the attachment was said to be through a carbon to carbon linkage rather than through the carboxyl group.

The amount of chemisorbed stearic acid at the highest solution concentration represents 0.365 and 0.626 of a monolayer at 30 and 25°C, respectively. If the molecular area is actually larger, as Graham and Hansen state it is, the values of q given in Appendix III are low and should be multiplied by 1.366, or 0.499 and 0.855 of a monolayer. Certainly the stearic acid molecule is not perpendicular to the surface, but rather is inclined and rotates so as to sweep out a conical space. This area would be difficult to calculate since the radius

Table 1

ADSORPTION DATA

Roebuck's Work	Total Adsorption (30°C.)		This Work	Total Adsorption (Tracer)	
Concentration Moles x 10^3	Gravimetric Moles x 10^{10}/cm^2	Tracer Moles x 10^{10}/cm^2	Concentration Moles x 10^3	30°C Moles x 10^{10}/cm^2	25°C Moles x 10^{10}/cm^2
15	13	13	7.5	122.1	148.0
7.5	8.4	7.8	3.0	88.5	108.3
3.75	5.6	5.4	1.0	69.5	100.7
1.5	4.3	3.8	0.7	54.2	78.6
0.375	3.4	2.9	0.4	33.4	49.3
			0.1	9.00	13.9
			0.05	3.90	6.40
	Chemisorption			Chemisorption	
15	3.6	0.2	7.5	2.96	5.08
7.5	3.5	0.2	3.0	2.77	4.58
3.75	3.1	0.17	1.0	2.40	4.21
1.5	3.7	0.17	0.7	2.00	3.88
0.375	3.7	0.1	0.4	1.37	3.23
			0.1	0.325	1.44
			0.05	0.182	0.764

The true surface areas used here are calculated using a roughness factor of 7.

of the circular path would decrease as the molecules were packed together more closely.

Mechanism of Chemisorption:

A possible mechanism for the chemisorption of stearic acid may be formulated based partially on the experimental evidence obtained in this work and partially on the theories given by Trapnell (11). The firmness with which the remaining stearic acid is held on the iron surface suggests that it is chemisorbed. Trapnell discusses the utilization of an available d orbital for chemisorption involving transitional metals. Iron has available d orbitals and could form a coordination complex between a metal atom at the surface and the acid molecule through the oxygen of the carboxyl group. Such a complex is not at all improbable and might lead eventually to compound formation in the form of an iron stearate. The formation of a compound between stearic acid on the surface and copper to give a copper stearate soap has been reported by Young (12). Bowden and Moore(13) also report the formation of salts when stearic acid is adsorbed on zinc, copper, and cadmium although there was none formed on adsorption on gold or platinum. In the cases of zinc, copper, and cadmium, reaction to form salts may be more direct since they have no available d orbitals. These can nevertheless form coordination complexes. There is no direct experimental evidence for the formation of an iron stearate on adsorption available however.

Potential-Time Behavior:

Adachi (14) finds potential-time curves similar to those shown in Figure 3, but makes no attempt to account for them. A hypothesis that would account for the maximum and minimum observed is not easily constructed. However, it is of interest to note that all of the curves in Figure 3 follow the same general pattern, whether stearic acid is present or not. The potential changes are, most likely, associated with changes of the metal surface brought about by standing in the solution. All that can be said with certainty at the present time is that the surface at the steady state is drastically different from the original one. The surface at the steady state is probably that of metallic substrate with an adsorbed layer; however, the nature of this adsorbed layer is not known. In acid solutions, hydrogen in some form is assumed to be chemisorbed. In neutral solutions, such as the ones employed in this work, hydroxyl might be adsorbed and furthermore, since in this case the solvent is mainly ethanol, it also may be adsorbed.

It is of interest to note that the potential obtained by simply immersing the electrode in the solution and allowing it to reach a steady state is the same, to within about $\pm$ 5 mv., as the potential observed after the electrode surface was reduced by cathodic pretreatment. In the latter instance, the electrode was polarized to the hydrogen evolution potential and hydrogen evolved for 30-60 minutes. The current was then stopped and the electrode allowed to reach a steady state as noted above. This coincidence of potentials suggests that an oxide layer was probably absent when electrodes simply immersed in the solution reached a steady state.

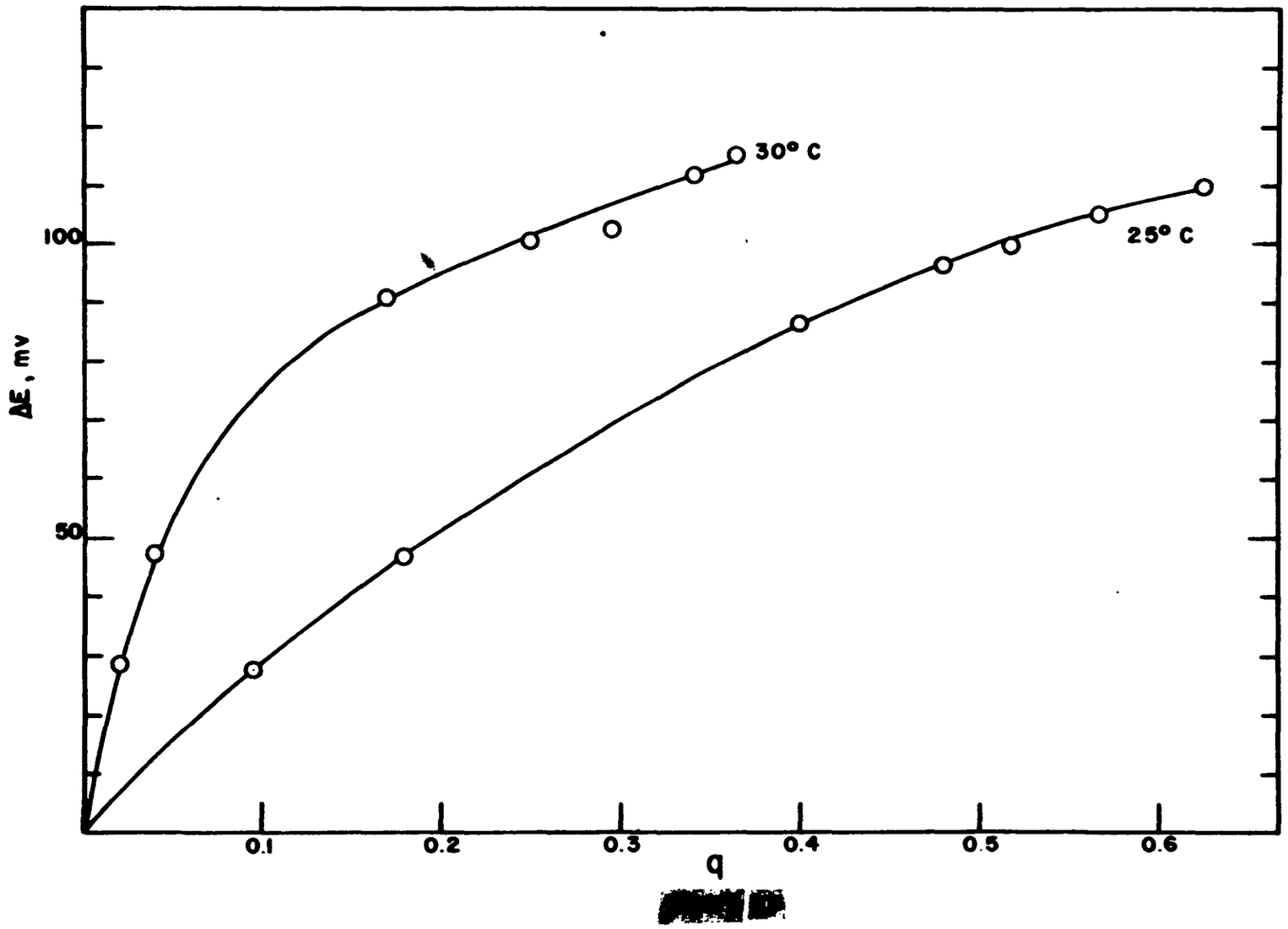

Potential change as function of coverage; q in monolayers.

Further evidence of the absence of an oxide layer at air-free steady state is the reversibility of the potential shift upon admitting oxygen to the system and then removing it. Oxygen was bubbled into the cell in place of helium after the steady state was attained under air-free conditions. The potential immediately moved in the noble direction. Oxygen was constantly bubbled into the system for 2 hours, during this time the potential become steady at a more noble value, Appendix II. Stopping oxygen flow and re-admitting helium caused the potential to return to its original steady state active value. The return took several hours and probably involved the same process as that occuring with a freshly immersed electrode.

If an oxide layer were present on the metallic substrate, the introduction of oxygen would not be expected to have any great effect on the potential. Curve B of Figure 4 is a steady state potential versus concentration of stearic acid plot for an oxygen saturated system at 25°C. Experiments were run to see if the order of introduction of oxygen and stearic acid was important, but there was no effect on the ultimate potential attained. The reversal of the potential to that of an air-free system upon re-admitting helium indicates that oxygen is not as strongly held as stearic acid. However, the oxygen does not appear simply to shift the curve in the more noble direction, but rather with stearic acid shows some synergistic character.

Potential-Concentration Behavior:

On adsorption of stearic acid from air-free solutions, the steady-state potential of the test electrode becomes more noble. Most of the potential shift in the noble direction occurs at stearic acid concentrations less than 10^{-3} M. At higher concentrations, the change is very gradual and the potential tends to come to a constant value. Similar results have been reported for steady-state potentials of steel in acid solutions containing various corrosion inhibitors (15, 16, 17). All potentials referred to hereafter are those for steady state.

Figure 8 suggests a close relationship between potential and extent of surface covered by chemisorbed stearic acid, and Figure 17 shows it more directly. A semilogarithmic chart of ΔE and q, yields satisfactory straight lines at both 25 and 30°C. (Figure 18). These are described by the following equation:

$$\Delta E = a + b \log q \qquad (1)$$

where a is the intercept when $q = 1$ and b is the slope. The values calculated for a and b by the least squares method are: at 25°C., $a = 129.3$ and $b = 103.1$; at 30° C., $a = 143.4$ and $b = 69.2$. The constant a is the theoretical potential change, ΔE, of an electrode completely covered by a monolayer of chemisorbed stearic acid at a given temperature. The slope b is $d(\Delta E)/d(\log q)$, the rate of change of potential in the noble direction as a function of coverage.

The above values of q are those calculated assuming a cross-sectional area for stearic acid of 20.5 A^2. On this basis, the leveling off of the potential,

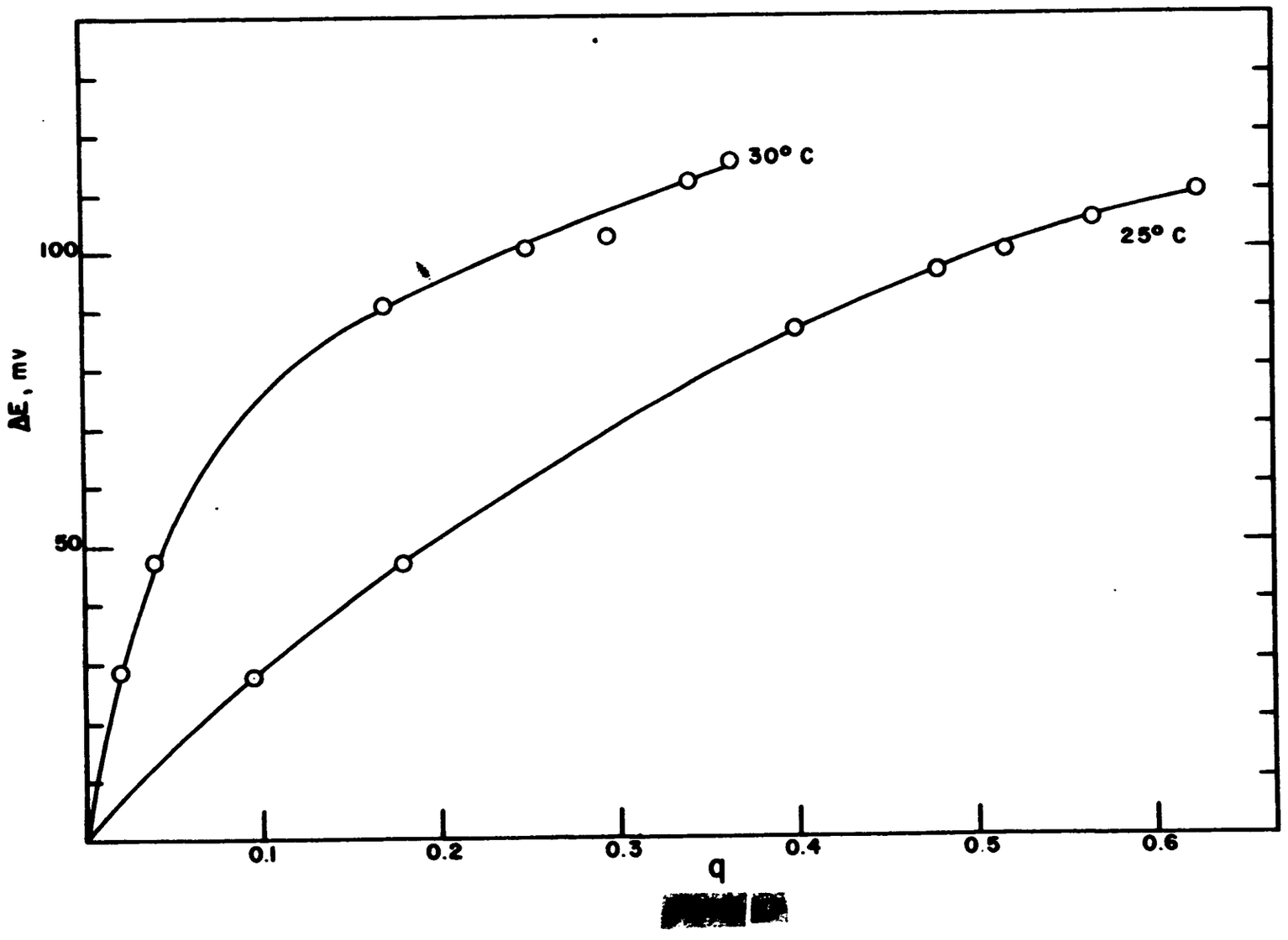

Potential change as function of coverage; q in monolayers.

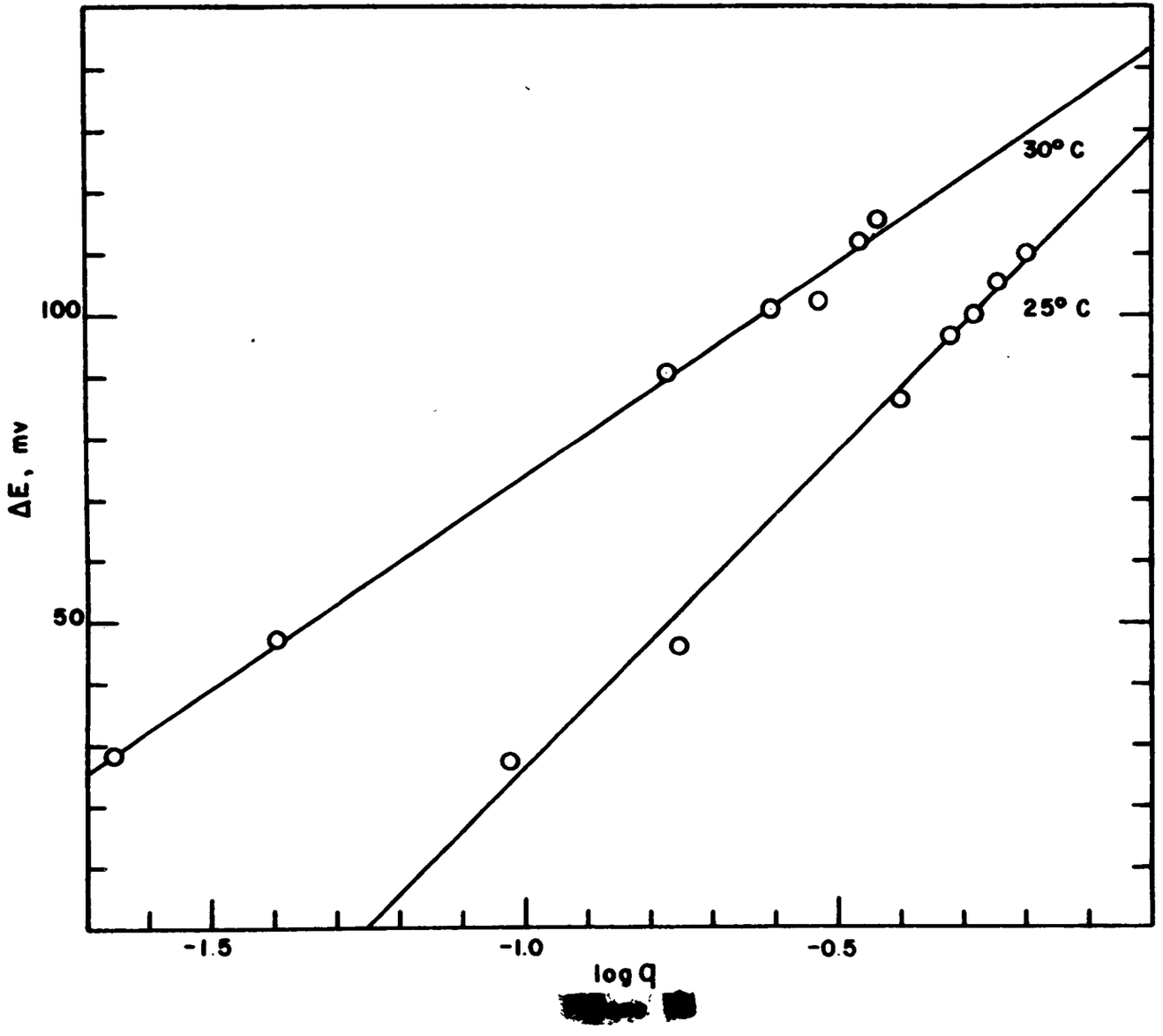
30° C
25° C
100
50
ΔE, mv
-1.5
-1.0
-0.5
log q

at 25°C., occurs when about half of the true surface is covered. The corresponding value at 30°C. is approximately 0.3 of a monolayer. As pointed out in the discussion of the adsorption isotherms, these values may be considerable higher if a cross-sectional area of 38 A^2 is used.

If these were equilibrium potentials, they should have a common point at q = 1 since ΔE automatically takes care of the temperature effect on the Nernst equation. However, these are not equilibrium potentials. The value of ΔE as a function of temperature is determined not only by the chemisorbed stearic acid but also by the effect of temperature on the anodic and cathodic overpotentials for the corrosion reaction occuring. Accordingly, the slope is probably a rather complicated function of temperature. Furthermore, on this basis, it is not necessary that a common point occur at q = 1. Considering these reasons and also that the adsorption data are for only two temperatures, it is impossible to extrapolate to 15°C. from potential measurements alone.

Polarization Studies:

The polarization studies are less conclusive than those of adsorption and open circuit potential, however some interpretations can be given them. Cathodic and anodic polarization curves for unbuffered neutral solutions over a range of stearic acid concentrations show that polarization of both reactions occurs with stearic acid present (Figure 9). The polarizing of both reactions increases as the concentration of stearic acid increases from 0 to 8 mM. This is what would be expected if stearic acid were a general type of inhibitor. It appears however from the curves that stearic acid polarizes the cathodic reaction to a slightly greater extent than it does the anodic reaction.

In the following discussion, consideration is given first to the cathodic curves and then to the anodic curves. Since these solutions were unbuffered neutral solutions, it is probable that concentration polarization is appreciable. As evidence of this, the potential would be expected to change markedly with stirring rate, rising as stirring rate decreased, and falling again as the stirring rate was increased. When the gas flow was decreased or stopped, the potential increased in the active direction for cathodic polarization. The gas flow rate was always maintained at the maximum practical rate. King (18) and Piontelli (19) each state that bubbling gas is not a very effective means of stirring.

An attempt was made to fit the data obtained from experiments in unbuffered neutral salt solutions to the Tafel expression:

$$E_o = a + b \log i \qquad (2)$$

where E_o is the overvoltage, the ΔE_c of Figure 9; a and b are constants; and i is the current density. Curves based on equation (2) are shown in Figures 10 and 12. Figure 14 is typical of the curves for solutions containing stearic acid, also see Appendix IV. The correction for concentration changes in H^+ and OH^- between the solution at the surface and the bulk of the solution as suggested by King (18) were made using the following equation:

$$\Delta E = \frac{-RT}{F} \ln \frac{a_1}{a_2} \qquad (3)$$

where a_1 and a_2 are the activities of a chemical specie in two different phases (1 and 2). The difference in OH^- concentration is the one to be considered in cathodic polarization since it Δ formed at the surface during the discharge of hydrogen ions. The change in OH^- is given by:

$$\Delta(OH^-) = 10^{-3}(\delta / D_{OH^-} F)\, i \qquad (4)$$

where δ is the thickness of the diffusion layer, D_{OH^-} is the diffusion coefficient, F is the Faraday, and $\underline{i}$ is the current density. Substitution may now be made in equation (3) and a value for the concentration overvoltage calculated:

$$\Delta E_{co} = \frac{-RT}{F} \ln \frac{(OH^-)b - 10^{-3}(\delta / D_{OH^-} F)i}{(OH^-)_b} \qquad (5)$$

where ΔE_{co} is the concentration overvoltage, $(OH^-)_b$ is the hydroxyl ion concentration in the bulk of the solution, δ, D_{OH^-}, $\underline{i}$, and F are given above This assumes the volume of the solution in the bulk to be of sufficient size that concentration changes in it are negligible. Concentration overvoltage corrections are subtracted from the experimental values of potential.

A correction for resistance overvoltage was considered by using the equation given by Barnartt (1):

$$E_r = 0.559\ ri/k \qquad (6)$$

where E_r is the resistance overvoltage, $\underline{r}$ is the radius of the capillary opening in the backside capillary of the electrode, $\underline{i}$ is again the current density, and k is the conductivity of the solution. The solution conductivity, except for those with acid and with buffer, was 1.12×10^{-2} ohm^{-1} cm^{-1}. The acid and buffer solutions had a conductivity of 1.38×10^{-2} and 1.24×10^{-2} ohm^{-1} cm^{-1} respectively. Using these values for k and r = 0.0175 cm., even at a current density of 200μA (the highest current densities used) the correction was less than 0.2 mv. Thus the latter correction could be neglected.

Using these corrections, it was still not possible to obtain straight line Tafel plots (Figures 11 and 13). Thus it is apparent that the overvoltage even in its corrected form does not fall in line with the existing ideas for aqueous systems. To determine whether or not polarization studies may be carried out effectively in neutral solutions of alcohol-water mixtures without buffer requires additional investigation.

In buffered solutions at pH = 6.5, concentration overvoltage appears to be less and straight line Tafel plots can be made for the higher current densities, but the slopes obtained are higher than they should be if only activation overvoltage is occuring, Appendix IV. A comparison of curves 4, 5, and 6 of Figure 14 with curve 1 of Figure 9 shows the decrease in concentration polarization brought about by the presence of buffer. The three buffers, acetic acid-sodium acetate (curve 4), propionic acid-sodium propionate (curve 5),

butyric acid-sodium butyrate (curve 6), gave curves which were essentially the same, as would be expected if there were no specific adsorption.

Concentration overvoltage does not appear to play a major role in the acid solutions, curves 1 and 2 of Figure 14. The plot of ΔE, overvoltage, against log i gives a straight line with a slope of approximately 0.1, Appendix IV. This is the slope that should be obtained for activation overvoltage in water according to Bockris (20). Curve 3 of Figure 14 is for a solution containing 8 mM stearic acid, 1 M $NaClO_4$, and 0.1 N $HClO_4$. This curve should fall to the left of the stearic acid-free curve since adsorption of stearic acid should polarize the cathodic reaction to some extent. This reasoning is based on the effects noted in unbuffered solutions. No explanation is available for this lack of polarization of the cathodic reaction for a solution containing stearic acid. The same stock solution was used for anodic polarization, and in this case the reaction was polarized by the presence of stearic acid.

Consider the relative positions of the curves for buffered solutions (4, 5, 6 of Figure 14), the curves for acid solutions (1, 2 of Figure 14), and the curve for unbuffered neutral sodium perchlorate solution (1 of Figure 9). The difference in potential between the two groups of curves, acid and buffered, is larger than might be expected from the difference in pH. This could be due to a small amount of concentration polarization as indicated by the slightly higher Tafel slope. It could also be due to adsorption of the buffer acids thus polarizing the electrode. The difference in potential between the curves with buffer and the one without buffer clearly indicate the effect of concentration polarization in the unbuffered solutions.

The anodic polarization curves in acid and buffered solutions show that concentration polarization probably is not the controlling factor. The only other observation made here about anodic polarization is that already stated, i.e., stearic acid in a solution of 1 M $NaClO_4$ and 0.1 N $HClO_4$ tends to polarize the anodic reaction to a noticeable extent.

The potential-time traces on anodic polarization shown in Figure 16 have also been seen by Stern (21) and Uhlig (22).

Summary

Adsorption isotherms for both total and chemisorption were obtained at 25 and 30°C. The fraction of the surface covered by the chemisorbed material was calculated in terms of a monolayer of stearic acid. Tracer techniques were used to determine the quantity of stearic acid adsorbed.

The use of d band character to explain chemisorption on metal catalysts has been applied here. It is postulated that stearic acid chemisorbs on iron and forms a surface coordination complex. Such a complex could lead to the formation of an iron soap.

Data were obtained showing the change in potential of an iron electrode as a function of the concentration of stearic acid at three temperatures (15, 25, and 30°C.). The change in potential with time from immersion to steady state was traced for several concentrations of stearic acid. All data were obtained in air-free systems except for one isotherm at 25°C. which was made in an oxygen-saturated system to determine the effect of oxygen on the potential. It was noted that the presence of oxygen enhanced the ennobling of the potential. The effect of increasing stearic acid concentration was to ennoble the open circuit potential of iron up to a certain point and there the effect became less, falling off to almost a horizontal straight line. The presence of oxygen and stearic acid together had an enhanced effect on the shifting of the iron potential in the more noble direction.

Relationships between the change in open circuit potential as a function of the surface coverage in monolayers for chemisorption were derived from the experimental data at 25 and 30°C.

Both cathodic and anodic polarization measurements were made in solutions of stearic acid with neutral salt present. In these, it was evident that stearic acid polarized both cathodic and anodic potentials to some degree. The effect of both concentration polarization and activation polarization was shown.

Similar studies were carried out in buffered solutions at pH of 6.5 and in 0.1 N $HClO_4$ at pH of about 1. In the buffered solutions the effect of pH was pointed out as was the reduced but still notable effect of concentration polarization. In the acid solutions, it was apparent that concentration polarization was small and the predominating factor was activation polarization.

Potential-time traces on application of two different anodic current densities were made. They conform favorably to the previously observed potential-time traces with the passage of anodic current.

References

1. Barnartt, S., J. Electrochem. Soc. 99, 549 (1952).

2. Eisenberg, M., Tobias, C. W., and Wilke, C. R., ibid. 102, 415 (1955).

3. Stephens, S. J., Dissertation, University of Texas (1953).

4. Hackerman, N. and Cook, E. L., J. Electrochem. Soc. 97, 1 (1950).

5. Hackerman, N., and Cook, E. L., J. Phys. Chem. 56, 524 (1952).

6. Roebuck, A. H., Dissertation, University of Texas (1951).

7. Morris, R. E. and Hollister, J. W., Ind. Eng. Chem. 40, 2325 (1948).

8. Kipling, J. J., J. Colloid Sci. 10, 156 (1955).

9. Vold, M. J., ibid. 7, 196 (1952).

10. Graham, D. and Hansen, R. S., J. Phys. Chem., 30th National Colloid Symposium, 1 (1956).

11. Trapnell, B. M. W., "Chemisorption", Academic Press Inc., New York, 1955. Chap. 7, pp. 170-75.

12. Young, J. E., Austrailian J. Chem. 8, 173 (1955).

13. Bowden, F. P. and Moore, A. C., Research (London) 2, 585 (1949).

14. Adachi, A., Tech. Reports of Osaka Univ. 5, 153 (1955).

15. Ch'jao, Shih-Jen and Mann, C. A., ibid. 39, 910 (1947).

16. Hoar, T. P., Trans. Electrochem. Soc. 76, 157 (1939); J. Electrochem. Soc. 99, 561 (1952).

17. Hackerman, N. and Sudbury, J. D., J. Electrochem. Soc. 93, 191 (1948).

18. King, C. V., J. Electrochem. Soc. 102, 193 (1955).

19. Piontelli, R., Z. Elektrochem. 55, 128 (1951).

20. Bockris, J. O'M., Ann. Review of Phy. Chem. 5, 477 (1954).

21. Stern, M. J., J. Electrochem. Soc. 102, 609 (1955).

22. Uhlig, H. H., Proc. of Natl. Acad. Sci. 40, 276 (1954).

Appendix I

Potential Change with Time

1.0M $NaClO_4$		1.0M $NaClO_4$ $4x10^{-5}$M S.A.		1.0M $NaClO_4$ $8x10^{-5}$M S.A.		1.0M $NaClO_4$ $2x10^{-4}$M S.A.	
time	Em(v)	time	Em(v)	time	Em(v)	time	Em(v)
1 min	-.484	1 min	-.459	1 min	-.459	1 min	-.458
2	-.512	2	-.471	4	-.503	2	-.470
3	-.542	3	-.480	5	-.520	3	-.480
4	-.555	7.5	-.520	7.5	-.543	4	-.485
5	-.568	10	-.540	10	-.560	5	-.492
7.5	-.579	15	-.559	15	-.550	7.5	-.500
10	-.575	20	-.567	20	-.526	10	-.505
15	-.565	25	-.560	25	-.505	15	-.509
20	-.560	30	-.547	30	-.488	20	-.504
25	-.553	35	-.531	35	-.480	25	-.500
35	-.542	40	-.517	40	-.476	30	-.493
40	-.533	45	-.504	45	-.476	35	-.487
44	-.528	50	-.498	50	-.478	40	-.480
50	-.526	55	-.497	60	-.481	45	-.476
60	-.528	60	-.500	70	-.484	50	-.472
70	-.534	65	-.503	80	-.489	55	-.469
80	-.544	75	-.508	90	-.490	60	-.466
90	-.548	90	-.513	100	-.494	65	-.462
100	-.552	100	-.516	110	-.497	70	-.460
110	-.555	110	-.522	120	-.500	80	-.461
130	-.558	120	-.527	130	-.504	90	-.462
140	-.554	140	-.527	140	-.508	100	-.464
16 hr	-.548	16 hr	-.524	16 hr	-.510	110	-.466
16.5	-.549	16.5	-.523	18	-.510	120	-.469
17	-.547	17	-.521	19	-.513	130	-.474
18	-.548	18	-.524	20	-.510	140	-.476
20	-.550	19	-.525	21	-.511	16 hr	-.483
21	-.549	19.5	-.527	22	-.508	17	-.483
22	-.546	20	-.526	23	-.508	18	-.481
23	-.548	20.5	-.524	24	-.510	19	-.482
23.5	-.550	23	-.524			20	-.481
24	-.548	23.5	-.525			21	-.480
24.5	-.548	24	-.524			22	-.484
						23	-.482

The European convention is used wherein the active potential is negative with respect to hydrogen and the saturated calomel electrode.

S.A. is used to abbreviate Stearic Acid.

Appendix I (cont'd.)

1.0M $NaClO_4$ 4×10^{-4}M S. A.		1.0M $NaClO_4$ 8×10^{-4}M S. A.		1.0M $NaClO_4$ 8×10^{-3}M S. A.	
time	Em (Volts)	time	Em (Volts)	time	Em (Volts)
1 min	-.398	1 min	-.420	1 min	-.374
2	-.416	2	-.432	2	-.392
4	-.446	3	-.441	3	-.410
5	-.456	4	-.446	4	-.430
7.5	-.480	5	-.449	5	-.444
10	-.500	10	-.460	7.5	-.453
15	-.520	15	-.466	10	-.449
20	-.510	20	-.462	15	-.442
25	-.496	25	-.455	20	-.438
30	-.480	30	-.446	25	-.432
35	-.470	35	-.440	30	-.427
40	-.464	40	-.434	35	-.423
45	-.458	45	-.428	40	-.419
50	-.456	50	-.424	45	-.418
55	-.457	55	-.422	50	-.414
60	-.457	60	-.418	55	-.412
70	-.462	68	-.415	60	-.411
80	-.466	75	-.418	65	-.412
90	-.470	80	-.420	70	-.413
100	-.472	90	-.426	80	-.416
110	-.473	100	-.430	90	-.418
120	-.471	110	-.436	100	-.420
130	-.469	120	-.444	110	-.422
140	-.466	130	-.452	120	-.426
16.5 hr	-.461	140	-.454	130	-.429
17	-.459	16 hr.	-.452	140	-.430
17.5	-.461	17	-.450	17 hr	-.439
18	-.460	18	-.450	18	-.436
18.5	-.462	19	-.452	19	-.438
19	-.461	20	-.451	20	-.435
19.5	-.462	21	-.452	21	-.436
20	-.459	23.5	-.450	22	-.438
21	-.460	24	-.450	23	-.437
24	-.462	24.5	-.450	24	-.437
25	-.462	25	-.450	25	-.436
26	-.460	25.5	-.452		
		26	-.449		

Appendix II

Steady State Potentials at Various Stearic Acid Concentrations and Different Temperatures

Air Free

Concentration Moles x 10^3	At 15°C.		At 25°C.		At 30°C.	
	ΔE(mv)	Em(v)	ΔE(mv)	Em(v)	ΔE(mv)	Em(v)
0	0	-0.545	0	-0.458	0	-0.552
0.01			8	-0.540		
0.04	12	-0.533	24	-0.524	32	-0.520
0.08	24	-0.521	38	-0.510	48	-0.504
0.20	50	-0.495	66	-0.482	77	-0.475
0.40	71	-0.474	87	-0.461	98	-0.454
0.50			92	-0.456		
0.60	77	-0.468	93	-0.455	105	-0.447
0.80	79	-0.466	97	-0.451	109	-0.443
1.00			100	-0.448		
8.00	89	-0.456	111	-0.437	125	-0.427

Oxygen Saturated at 25°C.

Concentration Moles x 10^3	At 25°C.	
	ΔE(mv)	Em(v)
0	130	-0.418
0.01	139	-0.409
0.08	170	-0.378
0.20	200	-0.348
0.40	228	-0.320
0.80	247	-0.301
8.00	300	-0.248

These values of ΔE represent the difference between the measured potential Em under the particular conditions given and the potential at 25°C. in an air-free system with no stearic acid present.

Appendix III

ADSORPTION

Concentration of Stearic Acid Moles x 10^3	Total Adsorption Moles x $10^{10}/cm^2$ 25°C	30°C	Chemisorption Moles x $10^{10}/cm^2$ 25°C	30°C	Surface Coverage in monolayers q 25°C	log q	q 30°C	log q
0.05	6.4	3.9	0.764	0.182	.094	-1.025	.022	-1.652
0.10	13.9	9.0	1.44	0.325	.177	-0.751	.040	-1.397
0.40	49.3	33.4	3.23	1.37	.398	-0.399	.168	-0.774
0.70	78.6	54.2	3.88	2.00	.478	-0.319	.247	-0.608
1.00	100.7	69.5	4.21	2.40	.518	-0.285	.295	-0.530
3.00	108.3	88.5	4.58	2.77	.565	-0.247	.341	-0.467
7.50	148.0	122.1	5.08	2.96	.626	-0.202	.364	-0.439

8.12×10^{-10} moles/cm^2 is one monolayer using a cross-sectional area of 20.5 $Å^2$ for stearic acid and a roughness factor of 7 for the iron surface.

Appendix IV

POLARIZATION

Cathodic						Anodic		
Solution: 1 M $NaClO_4$ (pH = 6.5)								
($i(\mu A/cm^2)$	log i	Em(v)	ΔE_c(mv)	ΔE_{co}(mv)	ΔE(mv)	$i(\mu A/cm^2)$	Em(v)	ΔE_a(mv)
Open Circuit		-0.548	0	0	0	Open Circuit	-0.548	0
8.68	-5.062	-0.886	338	150	188	8.76	-0.432	116
17.7	-4.763	-0.981	433	168	265	18.0	-0.382	166
43.6	-4.360	-1.110	562	191	371	44.1	-0.345	203
88.5	-4.053	-1.196	648	209	439	89.2	-0.302	246
121.6	-3.915	-1.218	670	217	453	122.3	-0.278	270
184.6	-3.734	-1.243	695	228	467	186.0	-0.236	312
Solution: 8 mM Stearic Acid + 1 M $NaClO_4$ (pH = 4.4)								
Open Circuit		-0.437	0	0	0	Open Circuit	-0.437	0
2.45	-5.610	-0.668	231	187	44	8.73	-0.192	245
5.37	-5.270	-0.790	353	193	160	17.8	-0.158	279
11.0	-4.960	-0.912	475	209	266	44.2	-0.119	318
27.9	-4.568	-1.074	637	232	405	89.7	-0.090	347
55.3	-4.258	-1.199	762	246	516	123.2	-0.075	362
74.5	-4.128	-1.247	810	257	553	187.7	-0.057	380
113.4	-3.944	-1.272	835	269	566			

Appendix IV (cont'd)

POLARIZATION

Cathodic						Anodic		
Solution: 0.8 mM Stearic Acid + 1 M $NaClO_4$ (pH = 5.5)								
$i(\mu A/cm^2)$	log i	Em(v)	ΔE_c(mv)	ΔE_{co}(mv)	ΔE (mv)	$i(\mu A/cm^2)$	Em(v)	ΔE_a(mv)
Open circuit		-0.451	0	0	0	Open Circuit	-0.451	0
8.77	-5.057	-0.619	168	209		8.78	-0.230	221
17.8	-4.748	-0.830	379	227	152	17.8	-0.195	256
43.3	-4.362	-1.036	585	250	335	44.3	-0.158	292
87.6	-4.056	-1.196	745	268	477	89.6	-0.129	323
120.9	-3.917	-1.259	788	276	512	123.2	-0.112	338
183.4	-3.736	-1.271	820	287	533	188.0	-0.086	367
Solution: 0.5 mM Stearic Acid + 1 M $NaClO_4$ (pH = 6.0)								
Open circuit		-0.456	0	0	0	Open Circuit	-0.456	0
8.68	-5.062	-0.748	292	179	113	8.80	-0.313	143
17.7	-4.752	-0.865	409	198	211	18.0	-0.255	201
43.6	-4.361	-1.016	560	220	340	44.4	-0.200	256
88.5	-4.053	-1.138	682	239	443	89.9	-0.155	301
121.8	-3.913	-1.179	723	257	466	124.0	-0.136	320
184.9	-3.733	-1.232	776	267	509	188.6	-0.107	349

Appendix IV (cont'd)

POLARIZATION

Cathodic				Anodic		
Solution: 0.1 N $HClO_4$ (pH = 1)						
$i(\mu A/cm^2)$	log i	Em(v)	ΔE_c(mv)	$i(\mu A/cm^2)$	Em(v)	ΔE_a(mv)
Open Circuit		-0.490	0	Open Circuit	-0.490	0
9.96	-5.002	-0.516	26	10.0	-0.482	8
20.1	-4.696	-0.533	43	20.3	-0.478	12
48.6	-4.314	-0.573	83	49.4	-0.469	21
95.8	-4.018	-0.609	119	97.8	-0.461	29
128.5	-3.891	-0.626	136	130.9	-0.458	32
188.1	-3.725	-0.642	152	191.6	-0.452	38
Solution: 0.1 N $HClO_4$ + 1 M $NaClO_4$ (pH = 1)						
Open Circuit		-0.618	0	Open Circuit	-0.618	0
9.97	-5.001	-0.637	19	9.97	-0.604	14
20.3	-4.692	-0.658	40	20.5	-0.598	20
50.0	-4.302	-0.699	81	50.8	-0.589	29
101.6	-3.994	-0.729	111	103.6	-0.581	37
139.9	-3.854	-0.743	125	141.3	-0.579	39
212.0	-3.674	-0.765	147	217.0	-0.577	41

Appendix IV (cont'd)

POLARIZATION

Cathodic				Anodic		
Solution: 8 mM Stearic Acid + 0.1 N $HClO_4$ + 1 M $NaClO_4$ (pH = 1.1)						
$i(\mu A/cm^2)$	log i	Em(v)	ΔE_c(mv)	$i(\mu A/cm^2)$	Em(v)	ΔE_a(mv)
Open Circuit		-0.496	0	Open Circuit	-0.496	0
8.72	-5.060	-0.507	11	8.83	-0.485	11
17.7	-4.752	-0.517	21	18.1	-0.476	20
43.7	-4.360	-0.543	47	44.6	-0.458	38
88.7	-4.052	-0.575	79	90.8	-0.441	55
122.5	-3.912	-0.592	96	125.2	-0.429	67
186.4	-3.730	-0.614	108	191.0	-0.427	69
Solution: 1 M $NaClO_4$ + Acetic acid-sodium acetate buffer (pH = 6.5)						
Open Circuit		-0.648	0	Open Circuit	-0.648	0
8.74	-5.059	-0.718	70	8.77	-0.639	9
17.8	-4.750	-0.788	140	17.9	-0.630	18
43.8	-4.359	-0.927	279	44.3	-0.607	41
88.4	-4.053	-0.978	330	89.9	-0.582	66
122.2	-3.913	-1.001	353	124.3	-0.569	79
185.6	-3.731	-1.031	383	188.8	-0.551	97

Appendix IV (cont'd)

POLARIZATION

Cathodic				Anodic		
Solution: 1M $NaClO_4$ + Propionic acid-sodium propionate buffer (pH = 6.5)						
$i(\mu A/cm^2)$	log i	Em(v)	ΔE_c(mv)	$i(\mu A/cm^2)$	Em(v)	ΔE_a(mv)
Open Circuit		-0.632	0	Open Circuit	-0.632	0
8.74	-5.059	-0.726	94	8.79	-0.619	13
17.8	-4.750	-0.855	223	17.8	-0.607	25
43.6	-4.350	-0.922	290	44.4	-0.586	46
88.4	-4.053	-0.976	344	90.2	-0.560	72
122.2	-3.913	-0.997	365	124.0	-0.542	90
185.6	-3.731	-1.026	394	188.9	-0.521	111
Solution: 1 M $NaClO_4$ + Butyric acid-sodium butyrate buffer (pH = 6.5)						
Open Circuit		-0.616	0	Open Circuit	-0.616	0
8.74	-5.059	-0.744	128	8.75	-0.596	20
17.8	-4.750	-0.854	238	18.0	-0.584	32
43.2	-4.365	-0.910	294	44.3	-0.560	56
88.8	-4.052	-0.957	341	90.1	-0.530	86
122.4	-3.912	-0.979	363	124.1	-0.510	106
186.0	-3.731	-1.006	390	190.0	-0.491	125

Appendix IV (cont'd)

POLARIZATION

Tafel Expression Slopes of Curves in Figure 17

Curve	Media	Slope
1	0.1 N $HClO_4$	.111
2	0.1 N $HClO_4$ + 1 M $NaClO_4$	.101
3	8 mM Stearic Acid + 0.1 N $HClO_4$ + 1 M $NaClO_4$	.111
4	1 M $NaClO_4$ + Acetic Acid-Sodium Acetate Buffer	.167
5	1 M $NaClO_4$ + Propionic Acid-Sodium Propionate Buffer	.168
6	1 M $NaClO_4$ + Butyric Acid-Sodium Butyrate Buffer	.149

DISTRIBUTION LIST FOR TECHNICAL REPORTS

Contract Nonr-375(02)

Corrosion Research Laboratory

Director, Naval Research Laboratory
Washington 25, D. C.
Attn: Code 2500, Metallurgy Division
Code 2020, Technical Library

Bureau of Aeronautics
Department of the Navy
Washington 25, D. C.
Attn: N. E. Promisel, AE-41 (2)
Technical Library, TD-41

Commanding Officer
Naval Air Materiel Center
Naval Base Station
Philadelphia, Pennsylvania
Attn: Aeronautical Materials Lab.

Bureau of Ordnance
Department of the Navy
Washington 25, D. C.
Attn: Re Technical Library, AD3 (3)

Superintendent, Naval Gun Factory
Washington 25, D. C.
Attn: Metallurgical Lab., DE 713

Commanding Officer
U. S. Naval Ordnance Laboratory
White Oak, Maryland

Commanding Officer
U. S. Naval Ordnance Test Station
Inyokern, California

Bureau of Ships
Department of the Navy
Washington 25, D. C.
Attn: Code 343 (2)
Code 337L, Tech. Library (1)
Code 347 (1)

Wright Air Development Center
Wright-Patterson Air Force Base, Ohio
Attn: Materials Laboratory (1)
Flight Research Laboratory (1)
(J. B. Johnson)

Bureau of Yards and Docks
Department of the Navy
Washington 25, D. C.
Attn: Research and Standards Division

Post Graduate School
U. S. Naval Academy
Monterey, California
Attn: Department of Metallurgy

Office of the Chief of Ordnance
Research and Development Service
Department of the Army
Washington 25, D. C.
Attn: ORDTB (3)

Commanding Officer
Watertown Arsenal
Watertown, Massachusetts
Attn: Laboratory Division

Commanding Officer
Frankford, Arsenal
Frankford, Pennsylvania
Attn: Laboratory Division

Office of the Chief of Engineers
Department of the Army
Washington 25, D. C.
Attn: Research & Development Branch

U. S. Air Forces
Research and Development Division
The Pentagon
Washington 25, D. C.

Chief of Staff, U. S. Army
The Pentagon
Washington 25, D. C.
Attn: Director of Research and
Development

U. S. Naval Engineering Experiment
Station
Annapolis, Maryland
Attn: Metals Laboratory

Director, Materials Laboratory
Building 291
New York Naval Shipyard
Brooklyn 1, New York
Attn: Code 907

Chief of Naval Research
Department of the Navy
Washington 25, D. C.
Attn: Code 423 (2)

Director
Office of Naval Research
Branch Office
346 Broadway
New York 13, New York

Director
Office of Naval Research
Branch Office
844 North Rush Street
Chicago 11, Illinois (2)

Director
Office of Naval Research
Branch Office
1000 Geary Street
San Francisco 9, California

Director
Office of Naval Research
Branch Office
1030 East Green Street
Pasadena 1, California

Assistant Naval Attache for Research
Office of Naval Research
Branch Office
Navy 100
c/o Fleet Post Office
New York, New York (2)

Carbide and Carbon Chemicals Division
Plant Records Department
Central Files (K-25)
Post Office Box P
Oak Ridge, Tennessee

Carbide and Carbon Chemicals Division
Central Reports and Information
Office (Y-12)
Post Office Box P
Oak Ridge, Tennessee

Director
Naval Research Laboratory
Washington 25, D. C.
Attn: Technical Information Center (6)

Commanding Officer
Office of Ordnance Research
Duke University
Durham, North Carolina
Attn: Metallurgy Division

Atomic Energy Commission
Division of Research
Metallurgical Branch
Washington 25, D. C.

National Bureau of Standards
Washington 25, D. C.
Attn: Physical Metallurgy Division

National Advisory Committee
for Aeronautics
1724 F. Street, N. W.
Washington 25, D. C.

Research & Development Board
The Pentagon
Washington 25, D. C.
Attn: N. C. Fick

Argonne National Laboratory
P. O. Box 5207
Chicago 80, Illinois
Attn: Dr. Hoylande D. Young

U. S. Atomic Energy Commission
1901 Constitution Avenue, N. W.
Washington 25, D. C.
Attn: B. M. Fry

Brookhaven National Laboratory
Information and Publication Division
Documents Section
Upton, New York
Attn: Miss Mary E. Waisman

Armed Services Technical Information
Agency
Documents Service Center
Knott Building
Dayton 2, Ohio (5)

General Electric Company
Technical Services Division
Technical Information Group
Post Office Box 100
Richland, Washington
Attn: Miss M. G. Freidank

Iowa State College
Post Office Box 14A, Station A
Ames, Iowa
Attn: Dr. F. H. Spedding

Knolls Atomic Power Laboratory
Post Office Box 1072
Schenectady, New York
Attn: Document Librarian

Los Alamos Scientific Laboratory
Post Office Box 1633
Los Alamos, New Mexico
Attn: Document Custodian

U. S. Atomic Energy Commission
New York Operations Office
Post Office Box 30, Ansonia Station
New York 23, New York
Attn: Division of Tech Information
and Declassification Service

Oak Ridge National Laboratory
Post Office Box P
Oak Ridge, Tennessee
Attn: Central Files

Sandia Corporation
Sandia Base
Classified Document Division
Albuquerque, New Mexico
Attn: Mr. Dale M. Evans

U. S. Atomic Energy Commission
Library Branch, Technical Information
Service, ORE
Post Office Box E
Oak Ridge, Tennessee

Westinghouse Electric Corporation
Atomic Power Division
Post Office Box 1468
Pittsburgh 30, Pennsylvania
Attn: Librarian

University of California
Radiation Laboratory
Information Division
Room 128, Building 50
Berkeley, California
Attn: Dr. R. K. Wakerling

Professor R. F. Mehl
Metals Research Laboratory
Carnegie Institute of Technology
Pittsburgh, Pennsylvania

Massachusetts Institute of Technology
Department of Metallurgy
Cambridge 39, Massachusetts
Attn: Prof. H. H. Uhlig

Professor P. Van Rysselberghe
University of Oregon
Eugene, Oregon

Professor A. T. Gwathmey
University of Virginia
Department of Chemistry
Charlottesville, Virginia

Professor P. Delahay
Louisiana State University
Baton Rouge, Louisiana

Professor W. D. Robertson
Department of Metallurgy
Yale University
New Haven, Connecticut

Professor H. J. Yearian
Physics Department
Purdue University
Lafayette, Indiana

Office of Naval Research
Navy Department
Washington 25, D. C.
Attn: Chemistry Branch, Code 425

Deterioration Prevention Center
2101 Constitution Avenue
Washington, D. C.
Attn: D. G. Greathouse

Professor G. Hill
University of Utah
Salt Lake City, Utah

Professor M. G. Fontana
Department of Metallurgy
Ohio State University
Columbus, Ohio

Mr. F. L. LaQue
International Nickel Company
67 Wall Street
New York, New York

Rock Island Arsenal
Rock Island, Illinois
Attn: H. L. Faigen

Office of Technical Services
Department of Commerce
Washington 28, D. C.

Dr. T. P. Dirkse
Department of Chemistry
Calvin College
Grand Rapids, Michigan

Professor F. O. Rice
Catholic University
Washington, D. C.
Attn: Contract NOrd-10260

Professor E. R. Allen
Department of Chemistry
Rutgers University
New Brunswick, New Jersey

Professor D. C. Grahame
Amherst University
Amherst, Massachusetts

Professor A. C. Zettlemoyer
Lehigh University
Bethlehem, Pennsylvania

Dr. Carl A. Zapffe
6410 Murray Hill Road
Baltimore, Maryland